EAWAG NEWS

Federal Institute for Water Resources
and Water Pollution Control

26/27

Swiss Federal Institutes of Technology

FEBRUARY 1989 - EAWAG, CH- 8600 DÜBENDORF, SWITZERLAND

COAGULATION OF SUBMICRON IRON OXIDE PARTICLES IN WATER

OXIDE SURFACE CHEMISTRY IN RELATION TO PARTICLE KINETICS

JAMES J. MORGAN

There is currently a heightened interest in the behavior of submicron ($<10^{-6}$ m size) colloidal particles in groundwaters, fresh waters and coastal environments. High specific surface areas make such small particles *potentially effective transport media for many trace elements*. Although physical models for submicron particle coagulation in the absence of strong repulsion forces (electrostatic or steric) are well developed (i.e, Brownian collision rates as described by Smoluchowski's equations for *fast* coagulation) reliable models for *slow* coagulation are still under development [1].

The recently completed doctoral research of Liyuan Liang [3] provides some insights into the role of *specific* chemical influences (pH, adsorbed anions and polyelectrolytes) on slow coagulation of small (70 nanometer diameter) iron oxide particles in water. Two aspects of that work are briefly reported here: the influences of pH and of adsorbed phosphate on rates of coagulation of colloidal hematite. Full details are available in Dr. Liang's thesis and will be found in future journal publications.

The relationship of hematite colloid stability to pH at 25°C is illustrated in Fig. 1, which shows the experimental stability ratio (W), potentiometrically-determined surface charge, and the electrokinetic mobility of 70 nm particles over the pH range from 3 to 11. The value W (or α^{-1}) gives the ratio of the transport-controlled ("fast") coagulation rate to the actual rate. At pH $\approx$8.5 (equal to H_{ZPC}, i.e. the pH of zero proton condition for suspended particles as e.g. colloidal particle) the stability ratio is unity for all ionic strengths (NaCl concentrations). At pH$\approx$5 and low ionic strength, coagulation is slowed down thousand-fold relative to that at pH_{ZPC}, a consequence of the high positive charge density from $>FeOH_2^+$ groups on the surface (compare σ and mobility data with W).

Specifically adsorbed anions, e.g. phosphate, affect stability strongly in a way that was anticipated on the basis of the phosphate species formed on an iron oxide surface when phosphate is adsorbed [2]. Fig. 2 shows that added phosphate causes strong variations in Fe_2O_3 stability, the effect depending upon pH. For example, at neutral pH, ten-fold variation in total phosphate first brings about colloid *destabilization* (W decreases from 50 to 2) and then *restabilization* (W increases to above 3000).

The coagulation kinetic patterns seen for pH and phosphate are representative of those also observed for other specifically-adsorbed monomeric anions (e.g.

Visiting scientists at EAWAG

In this number of EAWAG NEWS we asked some of the visiting scientists who have been in residence at EAWAG during 1988 to write short articles.

EAWAG is the only institution of its kind in Switzerland. We are dependent on the interaction and communication with institutions and scholars from abroad. Because of the small budget for visiting scientists, we have not been able to reimburse them adequately. In some cases we pay the travel costs, in others the apartment and only occasionally part of the living expenses. Nevertheless, we have been able to accomodate a large number of distinguished foreign scholars who mostly made personal financial sacrifices for coming to EAWAG. We have been profiting from their experiences and expertise; we also have been able to send our own scientists, engineers and students to their institutions.

By alloting some space to some of our visiting scientists, we would like to pay tribute to their scientific contributions, their support and friendship.

Werner Stumm

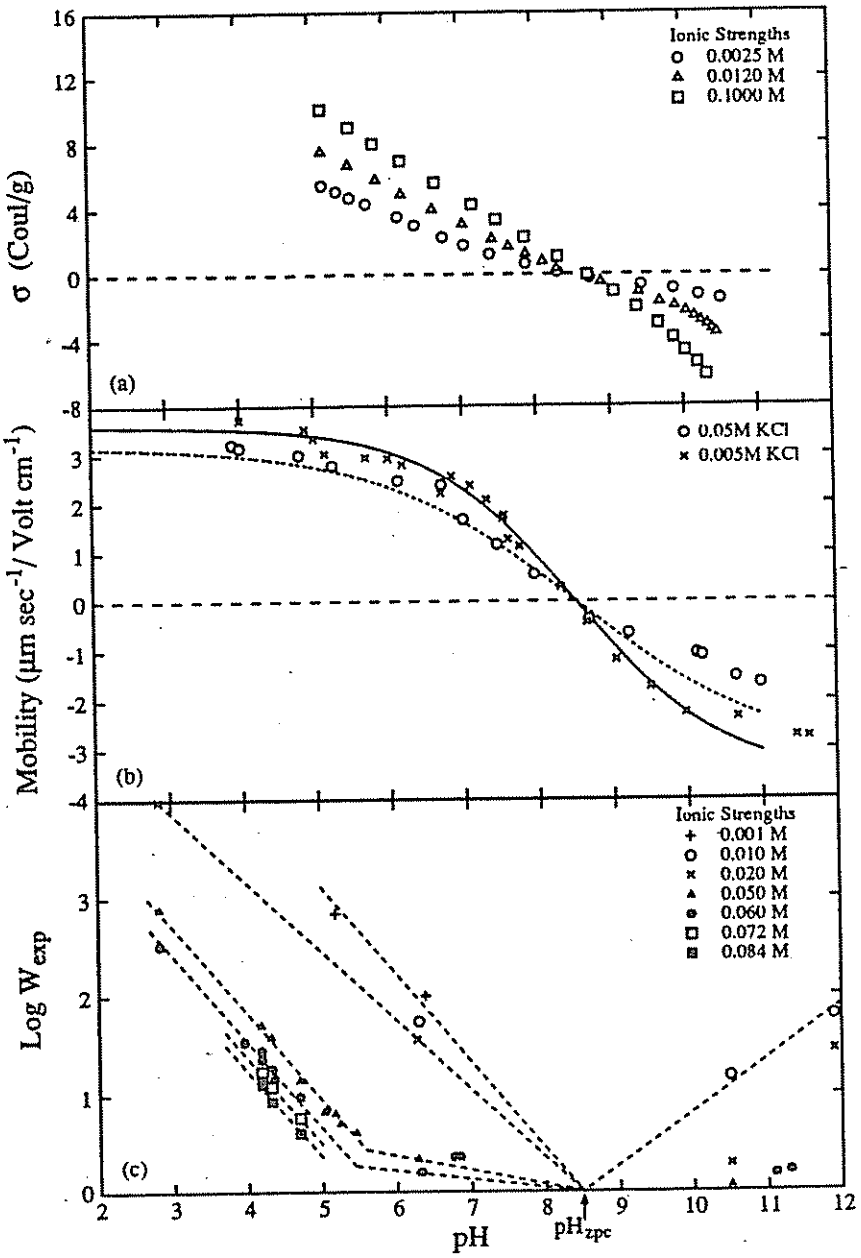

Fig. 1

Comparison of hematite surface charge, σ, mobility, and stability ratio, W_{exp}, as a function of pH. Note that at pH_{zpc} the net surface charge and mobility are both zero, and the stability is a minimum (Fig. 5.1 of [3])

The experimental stability ratio (W), the potentiometrically-determined surface charge, and the electrokinetic mobility of 70 nm particles over the pH range from 3 to 11 are shown.

phthalate or long-chain carboxylic acids) and for polymeric coagulant-dispersants (e.g. polycarboxylic acid, fulvic acid, humic acid.

Acid-base equilibria of the iron oxide surface and for solution species of anions, together with complex formation (ligand exchange) reactions at >FeOH surface sites account for strong surface charge variations and, in large part, for resulting changes in hematite particle stability. In addition, there is some evidence that steric factors (hydrophilic vs. hydrophobic orientation of adsorbed species) contribute to strong restabilization with excess adsorbate.

[1] O'Melia, C.R. Particle-particle Interactions. In: Stumm W. (ed): *Aquatic Surface Chemistry*, Wiley Interscience, New York,(1987).

[2] Stumm, W., Sigg L. Kolloidchemische Grundlagen der Phosphor-Elimination in Fällung, Flockung und Filtration. Z. für Wasser- und Abwasserforschung, *12*, 73-83, (1979).

[3] Liyuan Liang, Effects of Surface Chemistry on Kinetics of Coagulation of Submicron Iron Oxide Particles (α-Fe_2O_3) in Water, 1988, PhD thesis , Caltech, USA.

James J. Morgan *is Professor at the Department of Environmental Engineering Science at the California Institute of Technology, Caltech, Pasadena, California. He has been a frequent visiting scholar at EAWAG since 1971.*

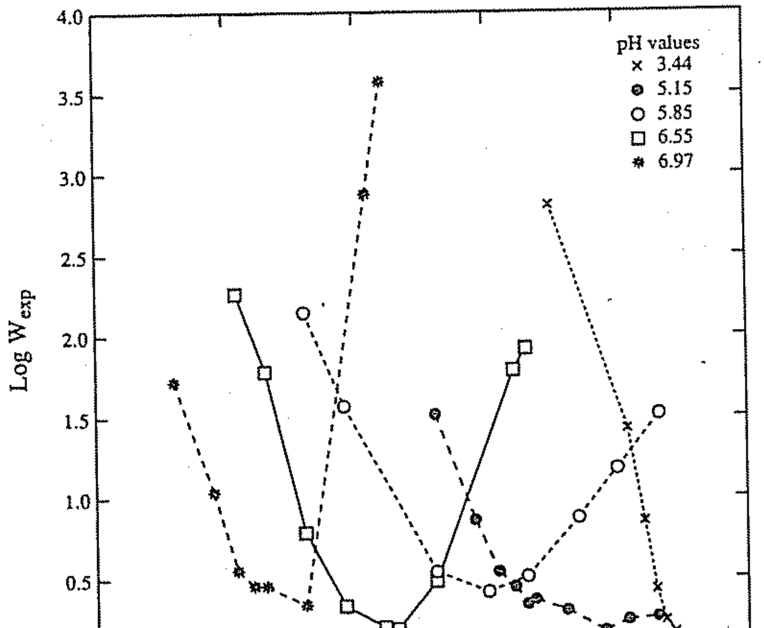

Fig. 2

Experimentally derived values of the stability ratio, W_{exp}, plotted as a function of NaH_2PO_4 concentration at various pH values (Figure 4.10 of [3]) The Fe_2O_3 concentration is 20 mg/l, the ionic medium 1mM NaCl, the temperature 25°C.

WHY SHOULD WE BE INTERESTED IN THE ADSORPTION OF HEAVY METALS BY ALGAL SURFACE?

XAN-BIN XUE

The ultimate fate of heavy metals in the environment is dictated by their affinity to particle surfaces. Thus, in natural water, particles settling into the sediments are essential carriers of metals into deeper water of lakes and oceans. A significant fraction of the settling particles may be of biotic origin (algae, biological debris). They provide a large number of surface sites with high affinity, because the cell surface containing polysaccharides and proteins consist of various functional groups, such as carboxylic, amino-, thio-hydroxo- and hydroxycarboxylic groups. Thus biological surfaces of settling materials play a dominating role in binding metal ions and other reactive elements, thereby regulating their residual concentrations. Models for the regulation of the concentration of heavy metals in oceans and lakes have been given by Whitfield and Turner [1] and Sigg [2,3].

The hypothesis has been proposed [1,2,4] that the Redfield Model of constant elemental composition of nutrients (N, P, C, Si, S) can be extended to those elements that are essential nutrients (Zn, Cu, etc.) and those that are mistaken by the cells as nutrients (such as Cd, As), the so-called "recycling elements". The approximate formula of algae for the ocean proposed by Morel and Hudson [4] is as follows

$$C_{106}H_{263}O_{110}N_{16}P_1(Fe,Ze,Mn)_{0.01}(Cu,Cd,Ni,etc.)_{0.001}$$

and Sigg [2,3] showed that the composition of algae in Lake Zurich can be approximated by the formula

$$(CH_2O)_{97}(NH_3)_{16}H_3PO_4Cu_{0.006}Zn_{0.03}$$

The binding of heavy metals in natural water depends on the relative affinity of these metals to the ligands in solution and the affinity to the surface sites of algae. The comparing of different possible scavenging phases with the calculated residence time ratios shows[4] that only biological materials can exhibit the high affinity required for the efficient metal scavenging, especially in deeper ocean. Furthermore, fluxes of Cu and Zn to the sediment in Lake Zurich [3] are higher in June-September, i.e. at times when biological meterials have important sedimentation, rather than in the fall and winter. These facts indicate that heavy metals are mainly associated with the biological materials and settle with them.

The interaction of metal ions with the surface of algae are probably also of importance in the bioavailability of heavy metals to the algae or in the toxicity effects. It has been well established that the bioavailability of most metal ions and their physiological or toxicological effects are primarily related to the activity of free metal ions. In fig. 1, I illustrate why this is so. The processes for the transportation of the metal ions in fig.1 have been described by Williams [5].

The arguments given illustrate how important it is to assess the adsorption of heavy metals to algae surfaces and to develop special methodology for measuring free metal ions. Especially sensitive methods such as voltammetry (including anodic stripping voltammetry), or especially developed ion selective electrodes which can be used without separation of the solid phase are needed. Fig. 2 exemplifies a set of titration curves for voltammetry to measure directly metal ions in solution in the presence of algae [6]. In order to be closer to lower levels of free ion concentration encountered in natural waters, we extended recently the methodology to

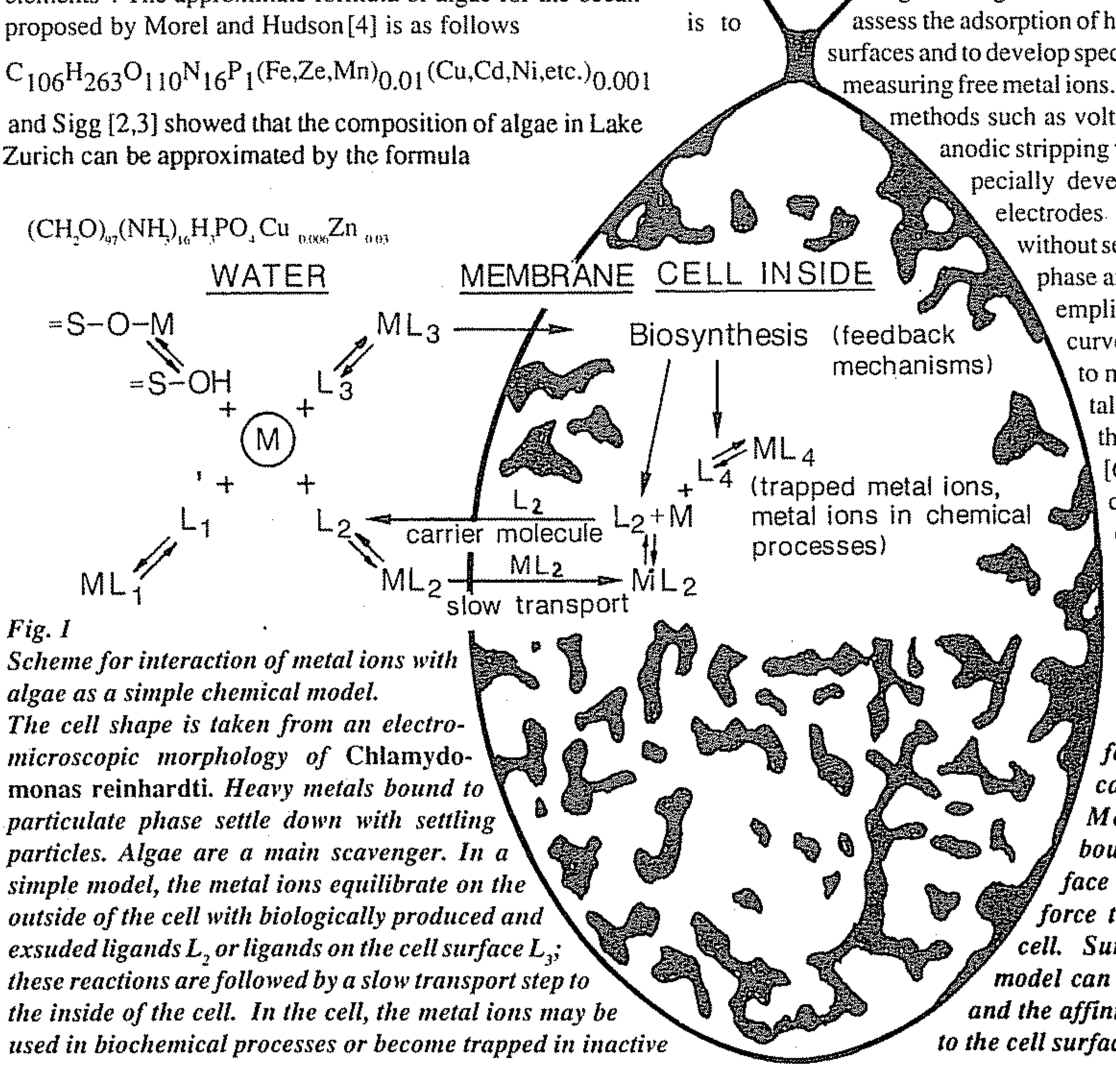

Fig. 1
Scheme for interaction of metal ions with algae as a simple chemical model.
The cell shape is taken from an electromicroscopic morphology of **Chlamydomonas reinhardti.** *Heavy metals bound to particulate phase settle down with settling particles. Algae are a main scavenger. In a simple model, the metal ions equilibrate on the outside of the cell with biologically produced and exsuded ligands L_2 or ligands on the cell surface L_3; these reactions are followed by a slow transport step to the inside of the cell. In the cell, the metal ions may be used in biochemical processes or become trapped in inactive forms by a detoxification mechanism. Metal complexes bound on the cell surface would be a driving force to the inside of the cell. Surface coordination model can describe the extent and the affinity of metal binding to the cell surface.*

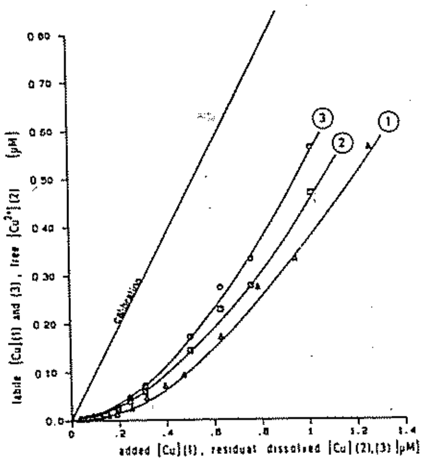

Fig. 2
Titration curves of algae with Cu(II) at pH 7. Concentration of algae, 12.8 mg (dry weight) l^{-1}
Curve 1, labelled Cu(II) as a function of added Cu(II); Curve 2, free [Cu^{2+}] as a function of total dissolved residual Cu(II) (corrected for loss); Curve 3, labelled Cu(II) as a function of dissolved residual Cu (II).

use metal ion buffers [Xue *et al.*, in preparation].

Our initial results on binding of heavy metals to algae surface, adsorption and uptake kinetics of Cu(II) and Cd(II), have been reported[6]. The results show that metal ion adsorption is consistent with a model in which the metal ion became in a first fast step coordinated to the algae surface, and subsequently became transferred in a slow step into the inside of the cell. The uptake kinetic curves show that a pseudo-equilibrium with the algae surface seems to be attained in a few minutes, and metal binding on the cell surface in form of surface complex formation with surface functional ligand groups occurs prior to the transport of the metals through membrane in the inside of cell. Thus, surface complex formation or adsorption equilibria, in principle similar to those discussed for oxide surface, can describe the extent and affinity of metal binding cell. Representative data are given in fig.3, in which the curves are calculated on the basis of two-site Langmuir model, the insert describing a considerable deviation from a linear relationship for the single Langmuir model at high coverage. If an interaction energy at the surface is taken into account because of the tendency of metal binding decreasing with increased metal loading of the algae surface, the surface complex formation equilibrium expression would be the constant capacitance model, so is the Flower Guggenheim Frumkin (FFG) model. The total capacities of metal binding on the cell surface of *Chlamydomonas*, estimated by FFG model, are 1.6×10^{-4} mol/g and 30 ions per nm^2 or 10^9 - 10^{10} metal ions per cell, respectively. These capacities are about one order of magnitude larger than that reported by Morel and Hudson [4]. The affinity of algae cell surface is similar to that observed earlier by Gonçalves *et al.* [7] on the interaction with bacterial cell suspensions, and appears to outweigh that observed for colloidal iron oxide of similar surface area.

[1] Whitfield M. and Turner D.R., in "Aquatic Surface Chemistry", Stumm W., Ed., (1987), pp. 457-493.
[2] Sigg L., in "Chemical Processes in Lakes", Stumm W., Ed., (1985), pp. 283-307.
[3] Sigg L., in "Aquatic Surface Chemistry", Stumm W., Ed., (1987), pp. 319-349.
[4] Morel F.M.M. and Hudson R.J.M., in "Chemical Processes in Lakes", Stumm W., Ed., pp. 251-281.
[5] Williams R.J.P., Phil. Trans. R. Soc. Lond. B 294, (1981), 57-74.
[6] Xue H.B., Stumm W. and Sigg L., Water Research, 22, (1988), 917-926.
[7] Gonçalves M.L.S., Sigg L., Reutlinger M. and Stumm W., Sci. Tot. Env., 60, (1986), 105-119.

Han Bin Xue *is Associate Professor at the Research Center for Eco-Environmental Sciences, Academia Sinica, in Beijing, China. She has been a visiting scientist at EAWAG in 1986 and since September 1988 on a leave from China. She has been collaborating with Prof. Werner Stumm and Dr. Laura Sigg.*

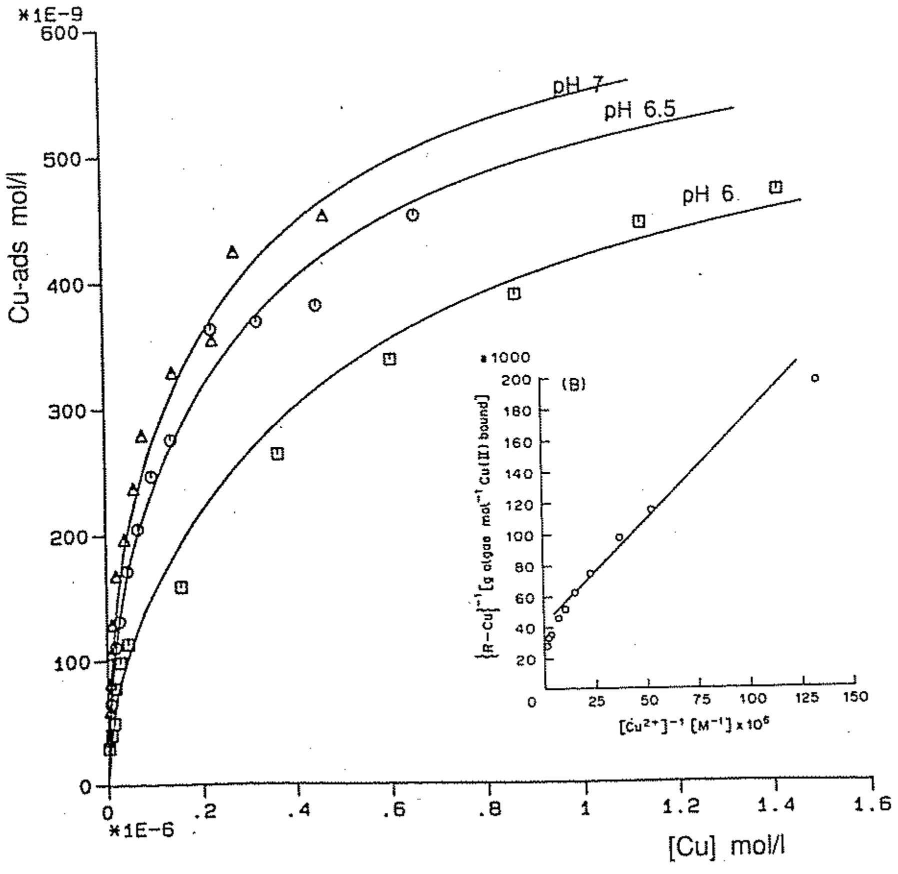

Fig. 3
The adsorption isotherms for the binding of Cu(II) to the algae surface at constant pH
The curves are calculated by two-site Langmuir equation. The insert shows the reciprocal forms of single Langmuir, the non-linearity is due to a decrease in binding tendency with increasing surface coverage. This can be corrected in more involved models.

FATE OF IRON AND ALUMINUM IN LAKE CRISTALLINA (SWITZERLAND)

JERALD SCHNOOR, RUDOLF GIOVANOLI, LAURA SIGG, WERNER STUMM, BARBARA SULZBERGER, JÜRG ZOBRIST

Acidic lakes and streams are often found in areas receiving acid deposition with sensitive geology and hydrology. Because of their crystalline rock geology and fast runoff, these natural waters have low concentrations of alkalinity and base cations (calcium, magnesium, sodium and potassium). Under the influence of increasing acidic deposition, neutralization by chemical weathering is often insufficient to prevent acidification (acid neutralizing capacities become less than zero). Aluminum and sometimes iron concentrations are elevated in these acid waters, and aluminum is toxic to fish and other aquatic organisms at concentrations greater than 4-8 μM liter^{-1} [1]. Also, aluminum is known to be toxic to fine roots of trees and may be one factor in forest decline[2]. Aluminum and iron oxides play an important role in the biogeochemical cycling of trace elements, especially metal ions and some nutrients[3]. Knowledge of the fate of iron and aluminum in acidic waters is important to understand the dynamics and health of ecosystems.

Fig. 1 is a schematic of the fate and transport of iron and aluminum through saturated groundwater in thin tills. Groundwater and streams transport dissolved ferrous iron and aluminum towards the lake. Some iron is lost via oxidation and precipitation along the way, and some aluminum is lost due to precipitation. Once to the lake, submicron particles of amorphous aluminum hydroxide sorb to sediments and are removed from the water column. However, aluminum hydroxide is subject to redissolution with decreases in pH due to snowmelt or rainfall runoff events.

Iron(II) has a more complicated story: Fe^{2+} that makes its way to the lake is subject to slow oxidation under acidic conditions. Once oxidized, it precipitates and settles to the bottom. In contrast to aluminum which sorbs throughout the sediments as submicron point flocs, the iron(III) hydroxides coagulate and form patches of clearly visible orange surficial sediments. Aluminum hydroxides are white, amorphous, and spread throughout the sediments; it is impossible to see $Al(OH)_3$ visually or to detect it via X-ray diffraction. Iron hydroxides are clearly visible through clear water, they are also amorphous to X-rays, and coagulate in flakes of a few mm in the largest dimension. The transformation of ferric hydroxide to goethite is strongly retarded by the presence of silicic acid, also present as a weathering product [4]. But ferric hydroxide can be re-reduced yielding soluble Fe^{2+}, and an iron cycle results that is coupled with metals and nutrient cycling (see Sulzberger et al.,see pages 18-22).

1. SITE DESCRIPTION

Lake Cristallina, at an elevation of 2400 m, in the southern alps of the Maggia valley, Tessin, Switzerland, provides an excellent opportunity to examine the relationship between chemical weathering, acid deposition, and the fate of iron(II) and aluminum in acidic waters. It lies above the tree-line with very thin soils and exposed bedrock over most of the watershed. Cation exchange and vegetation processes are relatively minor compared to forested ecosystems. Bedrock consists of granitic gneiss with steep slopes and granitic blocks in the upper portion of the catchment. The lake receives an average of 1.6 m per year of precipitation, mostly as snow, with an annual runoff of approximately 1.2 m[5]. The drainage area is 17 ha with a lake surface area of 0.75 ha and a mean hydraulic residence time of 1-2 weeks. The pH of precipitation is 4.85, with snow precipitation about pH 5.0 and rainfall pH 4.8 [6]. Dry deposition is not a large contribution to the total acid deposition, but there is evidence of some nitrate (HNO_3) deposition in the winter snowpack and sulfate (SO_2) deposition in the summer. Lake Cristallina has an average pH of 5.1, indicating partial neutralization of acidic deposition.

The primary reactions that serve to neutralize incident acid deposition are chemical weathering and nitrate assimilation/reduction. Principal minerals that contribute solutes to Lake Cristallina via chemical weathering reactions have been identified as plagioclase feldspars (30-45%), epidote (2-4%), biotite(8-14 %), and orthoclase (10-14, K-feldspar) [7]. Some calcite is believed to enter the catchment as wind-blown dust from nearby basins with exposed Triassic dolomite and calcareous shale (Bündnerschiefer).

2. REACTION KINETICS

Iron(II) that is liberated by biotite weathering reactions can be transported significant distances at low pH, even under aerobic conditions. Eventually iron(II) is oxidized to iron(III) hydroxides [8-10] which coagulate and become a part of the sediment. The overall oxidation reaction for Fe^{2+} can be written:

$$Fe^{2+} + 1/4\ O_2 + 2\ OH^- + 1/2\ H_2O \leftrightarrows Fe(OH)_3(s)$$

Kinetics of the reaction depend on the partial pressure of oxygen at saturation and the square of the hydroxide ion concentration according to the law of mass action.

$$d\{Fe^{2+}\}/dt = -\ k\{Fe^{2+}\}\{OH^-\}^2\ pO_2$$

> where k is the rate constant equal to 8 x 10^{13} min^{-1} atm^{-1} M^{-2} at 20 °C, t is time in minutes, and pO_2 is the partial pressure of oxygen (approximately 0.2 atm).

Kinetics of the reaction were first studied under conditions typical of natural waters by Stumm and Lee [9].

Oxides of aluminum and iron are subject to surface coordination reactions by hydrogen ions and organic ligands. Surface coordination of hydrogen ions or organic ligands is fast at the mineral surface. The rate determining step is the slow release of the "activated complex", that is the coordinated central metal ion with its ligands. Thus, the rate of reaction is dependent on the concentration or fraction of surface sites occupied by protons or coordinating ligands. For hydrolysis of oxides, the following rate equation has been proposed [11-13].

$$d\{M^{+n}\}/dt = k_h\ S\ \{\equiv\text{-}OH_2^+\}^n$$

> where k_h is the rate constant for attack by hydrogen ions, S is the surface area of the mineral, and the term in brackets is the activity of protons on the surface

raised to the power of the number of coordinating hydroxide ligands (the valence of the central metal ion in this case).

The hydrolysis reaction is not important for ferric hydroxide precipitates due to their low solubility, but it is critical for amorphous aluminum hydroxide. Submicron precipitates of $Al(OH)_3$ come into and out of solution very quickly with small changes in pH, due to their relatively high solubility in acidic waters and the large surface area associated with the amorphous phase. It is a surface controlled dissolution reaction. Aluminum hydroxide dissolution proceeds until saturation, and equilibrium expressions assuming control by natural gibbsite can often be employed[14.]

$$Al(OH)_3(s) + 3\,H^+ \leftrightarrows Al^{3+} + 3\,H_2O \qquad K=10^{+8.77}$$

At pH 5.1, the average number of hydroxide ligands associated with the aluminum complex ion is one, and in the range pH 5.2- 6.0, two hydroxide ligands are complexed predominantly. Aluminum toxicity to fish appears to be most severe in waters which are supersaturated with respect to $Al(OH)_3$ [15], and this is the case at Lake Cristallina [7].

3. SEM/TEM/EDX PHOTOMICROGRAPHS

Scanning Electron Microscopy (SEM), Transmission Electron Microscopy (TEM), and Energy Dispersive X-ray spectroscopy (EDX) were used to determine the most weatherable minerals in the catchment of Lake Cristallina for the geochemical mass balance. Fig. 2 shows feldspar and biotite crystals (Fig. 2a and 2c) that were the most weathered minerals found in sediments and rock fragments. Etch pits were pronounced on the surface of plagioclase grains, and they occurred in lines following crystal defects as well as randomly across the surface of the grain. An X-ray fluorescence spectrum of a quartz grain is shown in Fig. 2b, indicating an iron oxide covering that was observed visually and with SEM/EDX on some grains.

While several investigators have reported gibbsite solubility control in acidic waters, it has not been possible to demonstrate its existence using X-ray diffraction in northern temperate regions receiving acid deposition. Aluminum hydroxide that is formed is amorphous to X-rays. Another secondary weathering product, kaolinite, is also not detected. Apparently, temperatures are too cold and water transport too rapid for the formation of kaolinite even in groundwater, where pH and H_4SiO_4 concentrations are relatively high and kaolinite is supersaturated.

Fig. 3 is a scanning electron micrograph (element distribution map) of decomposed biotite platelets in the fine fraction of Lake Cristallina sediment. The Si and Fe maps show high densities of the elements indicating quartz-rich grains and ferric hydroxide precipitates, respectively. In contrast to Fe and Si, the element map for Al is mostly uniform over the entire scan, indicating precipitation of tiny particles of amorphous aluminum hydroxide throughout the sediment.

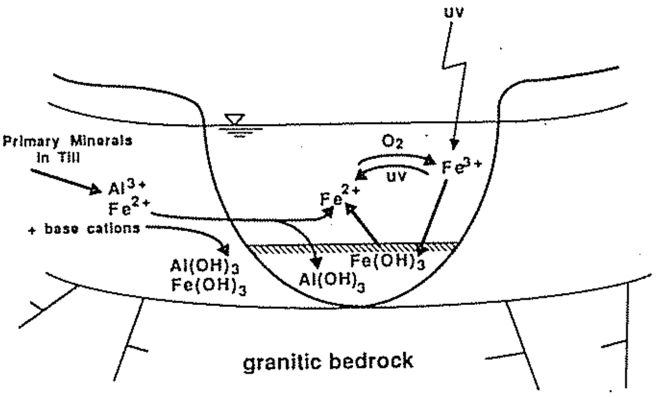

Fig. 1.
Fate of iron and aluminum in groundwater and acid lake water of an alpine catchment receiving acid deposition

4. SIMPLE MODELS

Simple mathematical models can be constructed to demonstrate the fate and transport of iron and aluminum in acid lake waters. For Fe^{2+}, the accumulation of mass in the lake is equal to the mass inflow minus the outflow mass discharge plus or minus the amount due to reactions (oxidation/precipitation, and reduction):

$$\underbrace{V\,(d\{Fe^{2+}\}/dt)}_{\text{accumulation}} = \underbrace{Q\{Fe^{2+}\}_{in}}_{\text{inflow}} - \underbrace{Q\{Fe^{2+}\}}_{\text{outflow}} - \underbrace{k_{ox}\{Fe^{2+}\}\{O_2(aq)\}\{H^+\}^{-2}V}_{\text{oxidation/precipitation}} + \underbrace{k_{red}\{>FeA-\}V}_{\text{reduction}}$$

where V = lake volume
Q = volumetric flowrate
$\{Fe^{2+}\}$in = inflow concentration from seepage/streams
k_{ox} = rate constant for oxidation = 3×10^{-13} min^{-1} $mol\ liter^{-1}$ at 5 °C
$\{O_2(aq)\}$ = dissolved O_2 concentration = 3.75×10^{-4} M
k_{red} = rate constant for Fe^{3+} reduction = f (I_o, pO_2, Fe^{2+})
$\{>FeA-\}$ = surface complex ligand concentration.

The rate constant for reduction of amorphous ferric hydroxides in sediments and lake waters, k_{red}, is negligible in Lake Cristallina. In grab samples, reduced iron concentrations have been less than detectable ($<5 \times 10^{-7}$ M). Upon irradiation of water with 4 kW/m^2 of white light containing 5 g $liter^{-1}$ of suspended solids collected from ferric hydroxide deposits in the surficial sediments of Cristallina, significant releases of Fe^{2+} were observed under air and nitrogen gas atmospheres. Sulzberger et al. (in this issue) discuss the reactions that can reduce iron hydroxides in the environment, including reductive dissolution by organic ligands which form surface coordination complexes, Fe^{2+} catalysis of hematite dissolution ,and photoreduction. The orange-colored ferric hydroxide flakes observed in surficial sediments of Lake Cristallina are exposed to sunlight through clear lake water (suspended solids concentration less than one mg $liter^{-1}$), but there is a paucity of coordinating ligands to serve as reductants at the surface of the mineral. (Dissolved organic carbon concentrations are on the order of 0.2 mg $liter^{-1}$.) The rate constant for ferric hydroxide reduction, k_{red}, is dependent on the light intensity, I_o, the partial pressure of oxygen which inhibits light-induced reduction, and the Fe^{2+} concentration itself, as an autocatalyst. When the reduction reaction is significant, a steady state concentration of Fe^{2+} will develop, and a diurnal cycle will be ob-

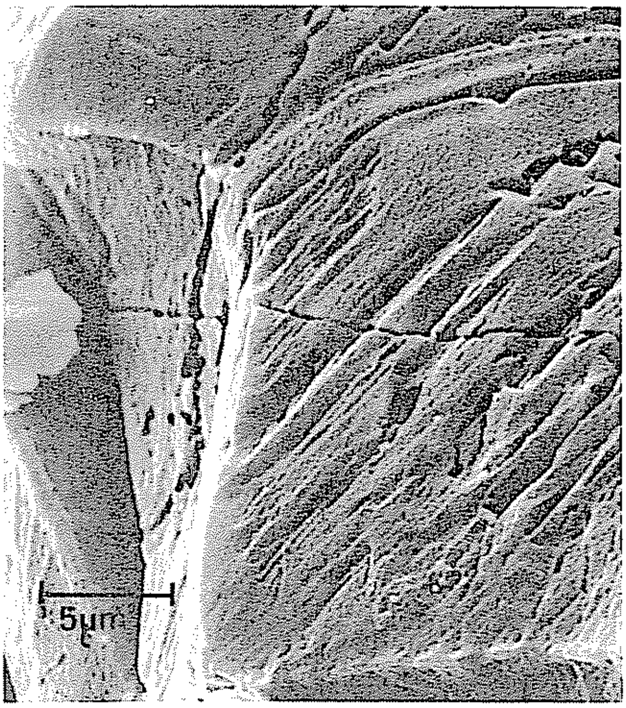

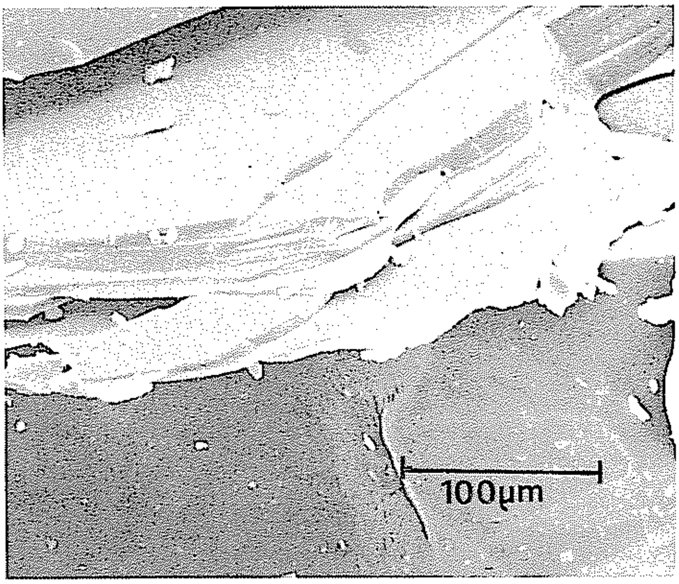

c) Scanning electron micrograph of a pack of mica platelets in the neighborhood of the feldspar of Fig. 2a The pack is attacked at the edges of the platelets.

Fig. 2

a) Etch pits on a feldspar crystal from the Cristallina catchment area. The grain is corroded. It is covered by a film of amorphous appearance. Since the grain was yellowish-brown to the naked eye, it can be assumed that this film is amorphous ferric hydroxide.

served if it is a photoreduction. Hydrous iron oxides absorb near-ultraviolet light and may serve as the reductant [16]. Under the assumptions of constant volume, steady state, and negligible Fe^{3+} reduction, the mass balance equation can be rearranged below. It is a first approximation to the fate of iron(II) entering an acidic lake such as Cristallina.

$$\{Fe^{2+}\} = \frac{\{Fe^{2+}\}_{in}}{(1 + k_{ox}\, t_o\, \{O_{2(aq)}\}\{H^+\}^{-2})}$$

where t_o = hydraulic detention time (13 days, Lake Cristallina)

Fig. 4 is a plot of the preceeding equation. The logarithm of the ratio of Fe^{2+} in the lake to Fe^{2+} in the inflow is given as a function of the hydraulic detention time and pH. It shows that lakes at pH 6 will not have detectable concentrations of reduced iron because the rate of oxidation is too rapid. It is not until the pH of lake is less than 5.0 that significant Fe^{2+} concentrations should be observed at detention times greater than 10 days. Because the presence of Fe^{2+} is favored with decreasing hydraulic detention time, elevated Fe^{2+} concentrations may occur more frequently in streams than in lakes.

5. OVERALL GEOCHEMICAL MASS BALANCE

The overall geochemical mass balance for the catchment at Lake Cristallina is the following, based on chemical analyses of precipitation and lake water from 1982-88:

$$Ca_6Mg_{0.5}Na_3K_2Fe_{2.5}Al_{12}Si_{25}O_{79.5} + 18\ H^+ + 123/2\ H_2O \leftrightarrows 3\ Na^+ + 2\ K^+ + 6\ Ca^{2+} + 1/2\ Mg^{2+} + 25\ H_4SiO_4 + 12\ Al(OH)_3(s) + 2.5\ Fe(OH)_2$$

Every liter of water passing through Lake Cristallina dissolves one micromole of the hypothetical aluminosilicate mineral. It serves to neutralize acidic deposition and release base cations, dissolved silica, amorphous aluminum hydroxide, and dissolved iron which is

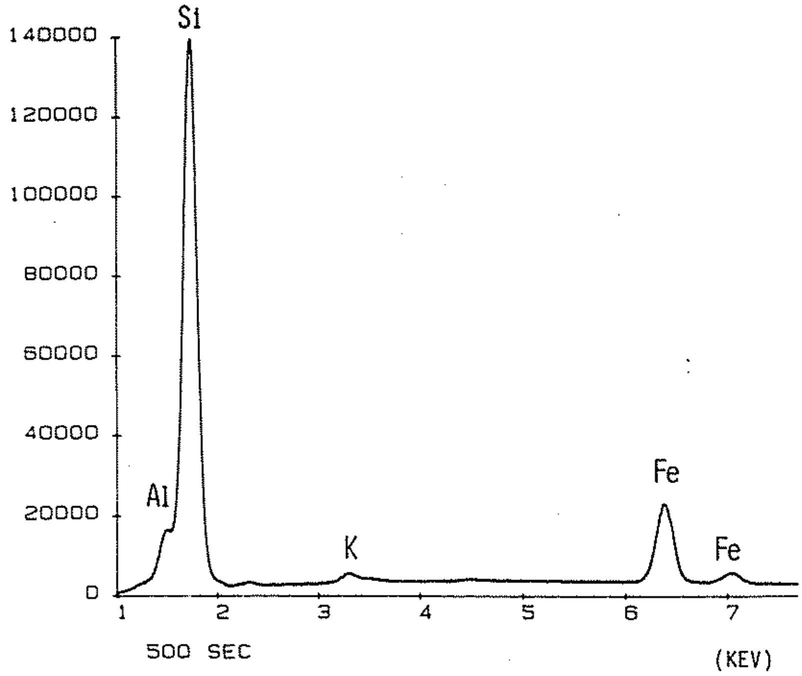

b) X-ray fluorescence spectrum taken in the scanning electron microscope on a quartz grain near the feldspar of Fig. 2A. The spectrum shows mainly Si and Fe, confirming that the brownish covering film is amorphous ferric hydroxide. Some K and Al also show up, presumably from a neighboring mica platelet.

subsequently oxidized to ferric hydroxide. About half of the $Al(OH)_3$ is redissolved and appears as inorganic aluminum in discharge waters. On a mass basis (kg ha^{-1} yr^{-1}), the overall reaction can also be written:

$$34 \text{ aluminosilicates} + 0.22\ H^+ + 13\ H_2O \rightarrow 0.8\ Na^+ + 0.9\ K^+ + 2.9\ Ca^{2+} + 0.14\ Mg^{2+} + 29\ H_4SiO_4 + 11\ Al(OH)_3 + 2.7\ Fe(OH)_2$$

The hydrogen ion deposition amounts to 224 eq $ha^{-1}yr^{-1}$ which is a threshold for acidification of the most sensitive lakes in northern temperate climates [18]. Of the 2.7 kg ha^{-1} yr^{-1} of $Fe(OH)_2$ that is released from weathering reactions, virtually all of it is oxidized and remains in the catchment, accounting for the formation of 3.2 kg ha^{-1} yr^{1} of solid ferric hydroxide in the soils and sediments. To a large extent, the geochemical mass balance, together with iron(II) oxidation kinetics, describes the fate of iron and aluminum in the catchment of Lake Cristallina.

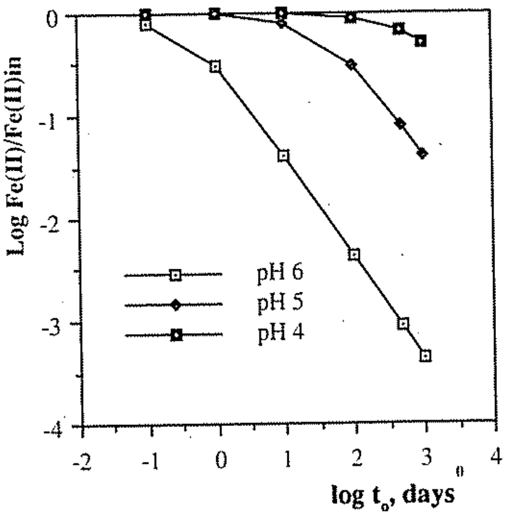

Fig. 4.
Log-Log plot of the calculated ratio of reduced iron concentration in a lake to the input concentration versus the hydraulic detention time and pH (According to equation given in the text). Lake of low pH (less than 5) and short detention time will contain significant Fe(II) concentrations due to slow iron oxygenation under these conditions.

6. CONCLUSIONS

Electron microscopy has helped to elucidate the weatherable minerals in the catchment of Lake Cristallina; they are feldspar grains of various mineralogy and biotite. The feldspar minerals provide calcium, sodium and potassium ions to the lake. Minor amounts of epidote (a hydrous silicate), $Ca_2(Al,Fe)_3(SiO_4)_3OH$ and trace quantities of windblown calcareous dust may also supply calcium to the water. Biotite provides a source of magnesium, potassium and reduced iron to groundwater and lakewater. Ferrous iron from biotite weathering is eventually oxidized, and it is determined spectroscopically in the sediments as amorphous ferric hydroxide flakes and as coatings on some mineral grains. Aluminum ions from aluminosilicate weathering reactions precipitate as submicron amorphous aluminum hydroxide, and these small particles are observed throughout the sediments. They are subject to rapid re-dissolution and precipitation depending on changes in pH of these acidic waters. Simple mathematical models indicate that lakes with pH≤5 may have signigicant steady state concentrations of Fe^{2+}. An overall geochemical mass balance results in 34 kg ha^{-1} yr^{-1} of rock weathering that neutralizes 224 eq ha^{-1} $yr^{-1}$of acidity and yields 3 eq ha^{-1} $yr^{-1}$of hydroxide and ≈ 6 eq ha^{-1} yr^{-1} of aluminum hydroxide. Future work will focus on the photoreduction of ferric hydroxide sediments and the steady state concentration of Fe^{2+}.

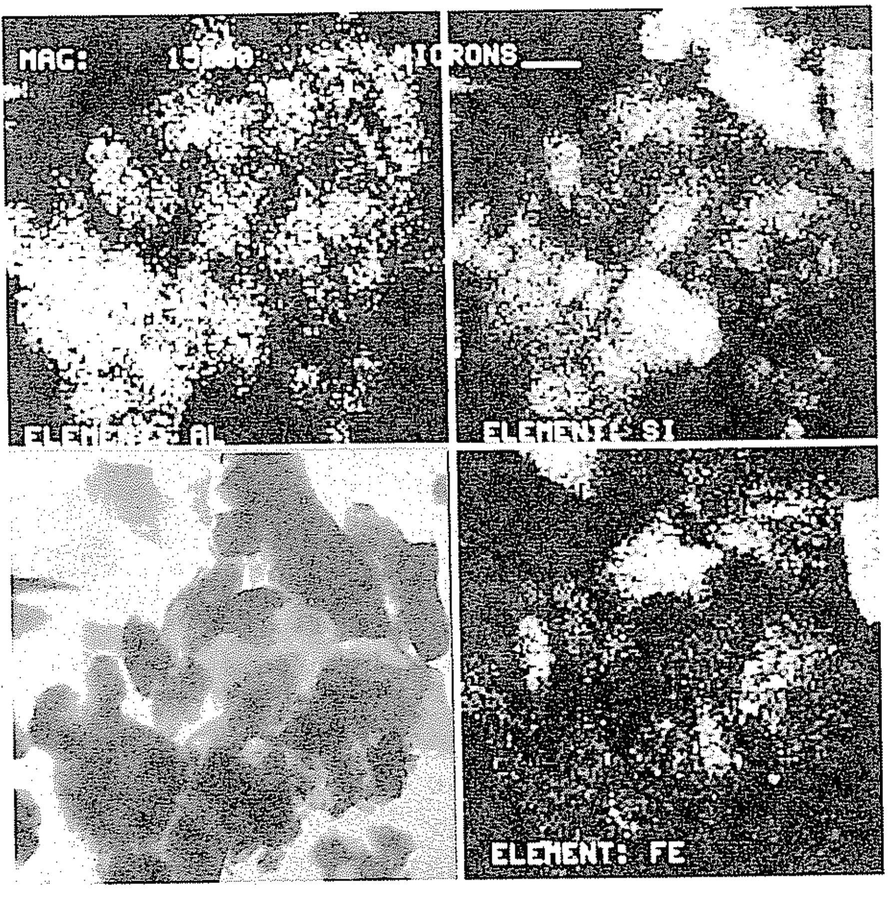

Fig. 3.

Element distribution maps for a sediment sample, taken in the transmission electron microscope in scanning mode. The elements Al, Si, Fe show themselves in their respective X-ray fluorescence radiation. The scanning transmission picture (bottom left) shows the analyzed region. The Si signal goes by and large with the contrast of the particles, while the Fe signal shows on the right hand side a pack of biotite platelets standing on edge, and in the rest of the picture, aggregations not corresponding to the image contrast of the reference picture (bottom left). The Al signal is even more evenly distributed all over the picture, indicating a mass of tiny particles of amorphous aluminum hydroxide.

[1] C.T. Driscoll and W.D. Schecher, Aluminum in the environment. In: Metal Ions in Biological Systems, Vol. 24, H.Sigel, A. Sigel (Eds.), Marcel Dekker, Inc., New York, 1988.

[2] B. Ulrich, Interaction of indirect and direct effects of air pollutants in forests. In: Air Pollution and Plants, C. Troyanowsky (Ed.), VCH Publishers, Deerfield Beach, Florida, 1984.

[3] J.R.White and C.T.Driscoll, Zinc cycling in an acidic Adirondack Lake, Environ. Sci. Technol., 21, 211-216, (1987).

[4] R.M.Cornell and R.Giovanoli, The influence of silicate species on the morphology of goethite (alpha-FeOOH) grown from ferrihydrite, Chem. Comm., J.Chem. Soc., London, 413, (1987).

[5] J. Zobrist et al., Buffering mechanisms in acidified alpine lakes. In: Reversibility of Acidification, H. Barth (Ed.), Elsevier Applied Science, Barking UK, 95-103, 1987.

[6] R. Mosello and G. Tartari, Effects of acid precipitation on subalpine lakes, Water Quality Bull., 96-100, (1983).

[7] R. Giovanoli et al., Chemical weathering of crystalline rocks in the catchment area of acidic ticino lakes, Switzerland, Clays and Clay Minerals, in press, (1988).

[8] W. Stumm and J.J. Morgan, Aquatic Chemistry, Second Edition, Wiley-Interscience, New York, 1981.

[9] W. Stumm and G.F. Lee, Oxygenation of ferrous iron, Industrial and Engineering Chemistry, 53, 143-46, (1961).

[10] P.C. Singer and W. Stumm, Science, 167, 3921, (1970).

[11] G. Furrer and W. Stumm, The coordination chemistry of weathering: I. Dissolution kinetics of delta-Al_2O_3 and BeO, Geochim. Cosmochim. Acta, 50, 1847-60, (1986).

[12] B. Zinder, G. Furrer, and W. Stumm, The coordination chemistry of weathering: II. Dissolution of Fe(III) oxides, Geochim. Cosmochim. Acta, 50, 1861-69, (1986).

[13] E. Wieland, B. Wehrli, and W. Stumm, The coordination chemistry of weathering: III. A generalization on the dissolution rates of minerals, Geochim. Cosmochim. Acta, 52, 1969-81, (1988).

[14] N.M. Johnson, Acid rain, dissolved aluminum and chemical weathering at the Hubbard Brook Experimental Forest, Geochim. Cosmochim. Acta, 46, 1421, (1981).

[15] J.P. Baker and C.L. Schofield, Aluminium toxicity to fish in acidic waters, Water Air Soil Pollut., 18, 289, (1982).

[16] D.M. McKnight, B.A. Kimball, and K.E. Bencala, Iron photoreduction and oxidation in an acidic mountain stream, Science, 240, 637-40, (1988).

[17] R.J. Hall et al., *Ecology*, 61, 976, Experimental acidification of a stream in the Hubbard Brook Experimental Forest, New Hampshire, (1980).

[18] J.L. Schnoor and W. Stumm, The role of chemical weathering in the neutralization of acidic deposition, Schweiz. Z. Hydrol., 48/2, 171-95, (1986).

Jerald L. Schnoor *is a professor and chairman of the Department of Civil and Environmental Engineering at the University of Iowa. He has been an active collaborator at EAWAG since 1982, having served sabbaticals in 1982 and 1988 and other short visits. Professor Schnoor is interested in modeling aquatic chemistry, particularly the fate and transport of pollutants in natural waters. Together with Professor Stumm and his EAWAG collaborators, he helped conceive and initiate the acid deposition research at Lake Cristallina in the Swiss Ticino Alps.*

Rudolf Giovanoli *is Professor at the Institute for inorganic, analytical and physical chemistry at the University of Berne. He is technical supervisor of the Laboratory of Electron Microscopy and has contributed in this function and also in the field of X-ray diffraction to EAWAG since 1973. His main interest is the reactivity of finely divided solids. Together with his EAWAG colleagues, he has investigated inorganic particulate matter in Lake Zurich, Lake Constance, and the acid lakes in Canton Ticino.*

PARTICIPANTS OF THE NINETH POSTGRADUATE COURSE IN SANITARY ENGINEERING AND WATER POLLUTION CONTROL (offered by the Institute of Aquatic Sciences, IGW, and the Institute for Hydraulics and Water Resources Management, IHW, of the ETHZ)

front row: *Franz Günter Kari, Ueli Spring, Annette Kuhn, Philipp Moosmann;* second row: *Felix Boecker, Hans Peter Hürlimann, Heinrich Adler, Gunnar Demoulin, Michael Ochs, Joachim Hanke,* third row: *Norbert Demuth, Christoph Bitterli, Reto Giulio Meuli, Gian Paul Calonder, Matthias Oplatka.*

COLLOIDAL STABILITY AND EUTROPHICATION

CHARLES R. O'MELIA AND ULRICH WEILENMANN

With hydraulic residence times ranging from months to years, lakes are efficient settling basins for particles. Lacustrine sediments are sinks for nutrients that support biological growth and for pollutants such as those toxic metals and synthetic organic compounds that associate with particulate matter. Research has been conducted jointly by investigators at the EAWAG and Johns Hopkins University on the significance of the effects that natural coagulation can have on particle sedimentation and water quality in lakes. Natural aggregation increases particle sizes and thus particle settling velocities, accelerates particle removal to the bottom sediments, and decreases particle concentrations in the water column. Results of this research have been published elsewhere [1, 2]. This report contains a short summary of the work and some comments about the origins and effects of colloidal stability in natural aquatic systems.

1. METHODOLOGY

The approach used in this research was to compare experimental evidence obtained from Swiss lakes with model simulations so as to evaluate effects that coagulation can have in lakes. In the course of this study attention was also directed towards the chemical factors that influence colloidal stability in natural waters.

The experimental aspects of this study were focussed on two hard-water lakes in Switzerland, namely, the northern basin of Lake Zürich and Lake Sempach. The hydraulic residence time of Lake Zürich is 1.2 years. Most of the particles in the lake are produced directly or indirectly by biological processes within the lake itself (e.g., photosynthesis, $CaCO_3$ precipitation). Phosphorus removal has been implemented in recent years at all wastewater treatment plants discharging into the lake; at present Lake Zürich can be described as between meso- and eutrophic. Lake Sempach has an average hydraulic residence time of 15.8 years; as in Lake Zürich, particles in the lake waters are primarily autochthonous. Phosphorus concentrations have increased substantially since about 1970 and the lake is eutrophic. Aeration and destratification have been introduced to prevent anoxic conditions in the hypolimnion and to reduce internal phosphorus cycling.

Experimental measurements in each lake included particle concentration and size measurements in the water column, sedimentation fluxes in sediment traps (by M. Sturm, EAWAG), and chemical and size characteristics of materials recovered from sediment traps. The colloidal stability of the particles in the lake waters was determined with laboratory coagulation tests. *Colloidal stability* was described by a stability ratio or attachment probability (α) defined as *the rate at which particles attach to each other divided by the rate at which they approach each other*. For a perfectly stable suspension, α=0; for a completely unstable one, α=1. Experimental procedures are described elsewhere [3-5].

Box models were used in a model to simulate particle transport in lacustrine systems that involve fluid flow, coagulation, and gravity. Each lake in summer was segmented into three well-mixed boxes corresponding to the epilimnion, thermocline, and hypolimnion. Particles in the lake waters were classified only by particle size in each lake compartment; typically about 25 size classes were used in each box. A differential equation for the rate of change in the number concentration of particles in

Fig. 1
Model simulations of particle volume concentrations in the summer as functions of the particle production flux in the epilimnion of Lake Zürich, adapted from [1].
Predictions are made for the epilimnion (A) and the hypolimnion (B). Simulations are made for input particle size distributions ranging from 0.3 to 30 µm described by a power law with an exponent of β. For β = 3, the particle size distribution of inputs peaks at the largest size, i. e., 30 µm. For β = 4, an equal mass or volume input of particles is in every logarithmic size interval [1, 8]. Two particle or aggregate densities (ρ_p) are considered, and a colloidal stability factor (α) of 0.1 is used. The broken line in (A) denotes predicted particle concentrations in the epilimnion when particles are removed from the lake only in the river outflow. Shaded areas show input fluxes based on the collections of total suspended solids in sediment traps and the composition of the collected solids.

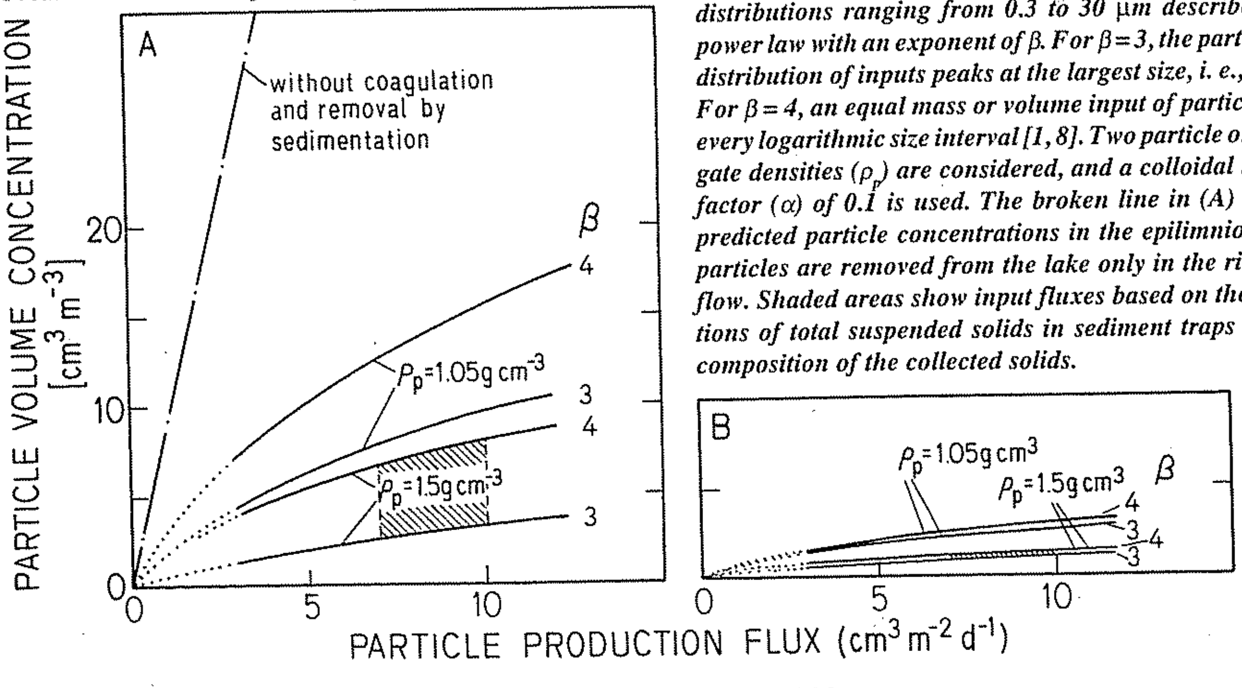

each size class in each box was written; for three lake compartments and 25 size classes, 75 equations resulted. These were integrated numerically to yield particle concentrations and sedimenting fluxes that varied in time and space. Coagulation removes particles from small size classes and introduces them into larger ones; the kinetics of coagulation followed the classic expressions of Smoluchowski [6] with gravity effects (differential sedimentation) as considered by Friedlander [7]. Sedimentation was described by Stokes' law in laminar conditions. Particles were assumed to be created in the lake by biological production and chemical precipitation. In addition to settling, they were removed from the lake by river discharge. Additional information about the modelling approach is provided elsewhere [4, 8, 9].

2. RESULTS AND DISCUSSION

Particle stabilities in Lake Zurich ($\alpha \approx 0.1$) and Lake Sempach ($\alpha \approx 0.01$) differed by about an order of magnitude, with the particles in Lake Sempach being more stable [1, 3]. Dissolved natural organic substances have been reported as stabilizing agents [e.g. 2, 10, 11] and divalent metal ions as destabilizing agents in aquatic systems. Both lakes contain appreciable and similar concentrations of calcium, about 1.2×10^{-3} M. The difference in colloidal stability between the two lakes is consistent with the difference in the concentrations of dissolved organic carbon (DOC) in these lakes. DOC is low in Lake Zurich, ~ 1 mg liter^{-1}; in Lake Sempach it is about 4 mg liter^{-1}. These results suggest that solution chemistry retards coagulation in Lake Sempach, reducing coagulation rate coefficients by an order of magnitude compared to Lake Zurich. The low particle stability (high attachment probability) in Lake Zurich favors coagulation, particle growth, and enhanced sedimentation.

Results of model simulations of effects of coagulation ($\alpha = 0.1$) and sedimentation at steady state in Lake Zürich during summer are presented in Fig. 1. Particle volume concentrations in the epilimnion and hypolimnion are plotted as functions of the particle production flux in the epilimnion. Biological degradation and chemical dissolution of particles are neglected in these calculations. Predicted particle concentrations are sensitive to the physical characteristics of the particles produced in the epilimnion, to their aggregation, and to their removal by sedimentation. Observed particle volume concentrations are 5-10 cm^3 m^{-3} in the epilimnion and ~ 1 cm^3 m^{-3} in the hypolimnion. Model simulations indicate that these concentrations can result from a particle production flux of 7-10 cm^{3}m^{-2} d^{-1} and a particle or aggregate density of 1.5 g cm^{-3}, in agreement with estimates from the sediment trap data. Aggregates with a density of 1.5 g cm^{-3} are considered to result from coagulation of calcite particles with phytoplankton. A particle production flux of 5 cm^3 m^{-2} d^{-1} in the epilimnion would produce, in the absence of particle removal by sedimentation assisted by coagulation, a particle volume concentration in the epilimnion of 43 cm^3 m^{-3} (Fig. 1), considerably in excess of observations. The model for coagulation and sedimentation used in this research provides a physical connection among particle production rates, deposition fluxes, and water column concentrations observed in Lake Zürich. In Lake Sempach, coagulation occurs and is important in establishing the decrease in particle concentration with depth observed from the epilimnion to the hypolimnion, but it is sufficiently slow that biological degradation and chemical dissolution of particulate materials exert substantial effects in reducing suspended concentrations and settling fluxes. The origin of this slow coagulation rate in Lake Sempach lies in solution chemistry and specifically in the high DOC concentration in the lake water.

3. COLLOIDAL STABILITY

The enhanced stability of natural particles in natural waters containing natural organic matter is a consistent observation without a clear cause. Some speculation is presented here. Humic substances comprise the principal fraction of dissolved organic matter in most natural waters. These molecules can be considered as flexible polyelectrolytes with anionic functional groups [12]; they also have hydrophobic components. In fresh waters such molecules assume extended shapes due to intramolecular electrostatic repulsive interactions. When adsorbed at interfaces at low ionic strength, they assume flat configurations [13]. Adsorption on inorganic surfaces such as metal oxides could result from the ligand exchange of functional groups on the humic substances (carboxylic, phenolic) with surface hydroxyl groups on the metal oxides, supplemented by a hydrophobic interaction involving nonpolar components of the humic molecules. The result would be an accumulation of negative charge on the surface of the oxide due to the adsorbed organic substances. At low ionic strength the Debye length (diffuse layer thickness) could exceed the thickness of the flat adsorbed organic layer and the particles would be stabilized electrostatically. The <u>origin</u> of the stabilization is in the chemical and hydrophobic interactions between the humic substances, the water, and the surface; the <u>effect</u> of these interactions is an electrostatic type of stabilization of the particles. In this perspective, calcium ions could interact specifically with functional groups on the adsorbed molecules, reducing the net charge on the particle; a reduction in the range of diffuse layer interactions would also occur. A decrease in particle stability (increase in α) would result. For organic surfaces such as algal cells and detritus, the process would differ somewhat, but particle stability would again involve adsorption of anionic natural organic substances through specific chemical and hydrophobic interactions to produce negatively charged particles that are stabilized primarily by their charge.

Humic substances in lakes can result from autochthonous biological processes within the lake and from allochthonous inputs from terrestrial sources. The macromolecular biological debris produced by biological wastewater treatment plants can have chemical and physical characteristics similar to natural organic substances and might provide a source of stabilizing organic matter when discharged into lakes.

4. CONCLUSIONS

Results of experimental measurements and mathematical modelling demonstrate that coagulation in lakes can be sufficiently rapid and extensive to affect suspended particle concentrations and sedimenting fluxes significantly. The process dominates particle removal in Lake Zürich and substantially influences particle concentrations in the water column of Lake Sempach.

THE INFLUENCE OF AMMONIA ON THE OXIDATION OF AQUEOUS SULFUR DIOXIDE IN ATMOSPHERIC DEPOSITION

PHILIPPE BEHRA, LAURA SIGG, AND WERNER STUMM

1. INTRODUCTION

It is well known that oxides of sulfur and nitrogen emitted into the atmosphere are converted by various oxidative pathways in the gaseous and aqueous phases into sulfate and nitrate. With regards to SO_2, this transformation is relatively fast in the aqueous phase and occurs there primarily [1, 2]. On the other hand, the rate of oxidation of nitrogen oxide occuring fast in the gaseous phase is considered to be slow in the aqueous phase. Since these oxidation reactions are accompanied by a generation of protons, the aqueous phase becomes acidic: the overall process is termed acid deposition [2].

Although emissions of ammonia are able to neutralize part of the aqueous acidity, NH_3 has consequences by affecting the rate of SO_2 oxidation and thus the H_2SO_4 generation; furthermore, any NH_3 deposited on soils adds to soil acidification by becoming eventually converted into HNO_3 by microbially mediated nitrification.

The importance of NH_3 in the atmosphere and its role in acid deposition and indirect effects on the oxidation of SO_2 have been recognized by various authors [3, 4]. Our interest in the role of NH_3 in acid deposition was stimulated by measurements of the chemical composition of fog and aerosols, and the assessment of factors that regulate their composition [5, 6, 7].

Although the source functions of NH_3 and SO_2 showed considerable variations, remarkably constant molar proportions of NH_4^+ and SO_4^{2-} have been observed in fogwater during events

---

Natural coagulation in lakes is a process that is strongly influenced by solution chemistry. Calcium ions act as destabilizing agents and enhance natural coagulation while dissolved natural organic matter stabilizes particles and retards coagulation. Since solution chemistry varies widely among lakes, natural coagulation rates are expected to vary widely among lacustrine systems. Field observations of Lakes Zurich and Sempach support this view. Although primary productivity in Lake Zürich is considerably lower than in Lake Sempach, higher sedimenting fluxes are observed in Lake Zürich. The waters of Lake Zürich are low in dissolved organic carbon, permitting rapid coagulation in the epilimnion of the lake and producing correspondingly rapid sedimentation rates. Colloidal stability can be a factor in eutrophication [1].

So, the sources of DOC in lakes merit identification, as well as the extent to which eutrophication can be influenced by the persistent organic substances that are residues of biological activity in otherwise efficient wastewater treatment facilities.

[1] U. Weilenmann, C. R. O'Melia and W. Stumm: Particle transport in lakes: Models and measurements, Limnology and Oceanography, *34*, 1-18 (1989).

[2] W. Ali, C. R. O'Melia and J. K. Edzwald: Colloidal stability of particles in lakes: Measurement and significance, Water Science and Technology, *17*, 701-712 (1985).

[3] U. Weilenmann: The role of coagulation for the removal of particles by sedimentation in lakes, Ph.D. thesis No. 8018, Eidgenössische Technische Hochschule Zürich, 163 p. (1986).

[4] W. Ali: Chemical aspects of coagulation in lakes, Ph.D. thesis, The Johns Hopkins University, 222 p. (1985).

[5] L. Sigg, M. Sturm and D. Kistler: Vertical transport of heavy metals by settling particles in Lake Zürich, Limnology and Oceanography, *32*, 112-130 (1987).

[6] M. von Smoluchowski: Versuch einer mathematischen Theorie der Koagulationskinetik kolloider Lösungen, Zeitschrift für physikalische Chemie, *92*, 129-158 (1917).

[7] S. K. Friedlander: Smoke, Dust and Haze, Wiley-Interscience, New York, 317 p. (1977).

[8] D. F. Lawler, C. R. O'Melia and J. E. Tobiason: Integral water treatment plant design: From particle size to plant performance, In Particulates in water: Characterization, fate, effects, and removal, M. C. Kavanaugh and J. O. Leckie (Eds.), Advances in Chemistry Series No. 189, American Chemical Society, Washington, D. C., 353-388 (1980).

[9] C. R. O'Melia and K. S. Bowman, Origins and effects of coagulation in lakes, Schweizerische Zeitschrift für Hydrologie, *46*, 64-85 (1984).

[10] E. Tipping and D. C. Higgins: The effect of adsorbed humic substances on the colloidal stability of haematite particles, Colloids and Surfaces, 85-92 (1982).

[11] R. J. Gibbs: Effect of natural organic coatings on the coagulation of particles, Environmental Science and Technology, *17*: 237-240 (1983).

[12] P. K. Cornel, R. S. Summers and P. V. Roberts, Diffusion of humic acid in aqueous solution, Journal of Colloid and Interface Science, *110*: 149-164 (1986).

[13] J. Lyklema and G. J. Fleer: Electrical contributions to the effect of macromolecules on colloid stability, Colloids and Surfaces, *25*, 357-368 (1987).

Charles R. O'Melia is a Professor in the Department of Geography and Environmental Engineering at The Johns Hopkins University in Baltimore, Maryland, U. S. A. He has been a visitor and collaborator at EAWAG since 1971, and is spending the 1988-89 academic year on sabbatical leave at the Institute.

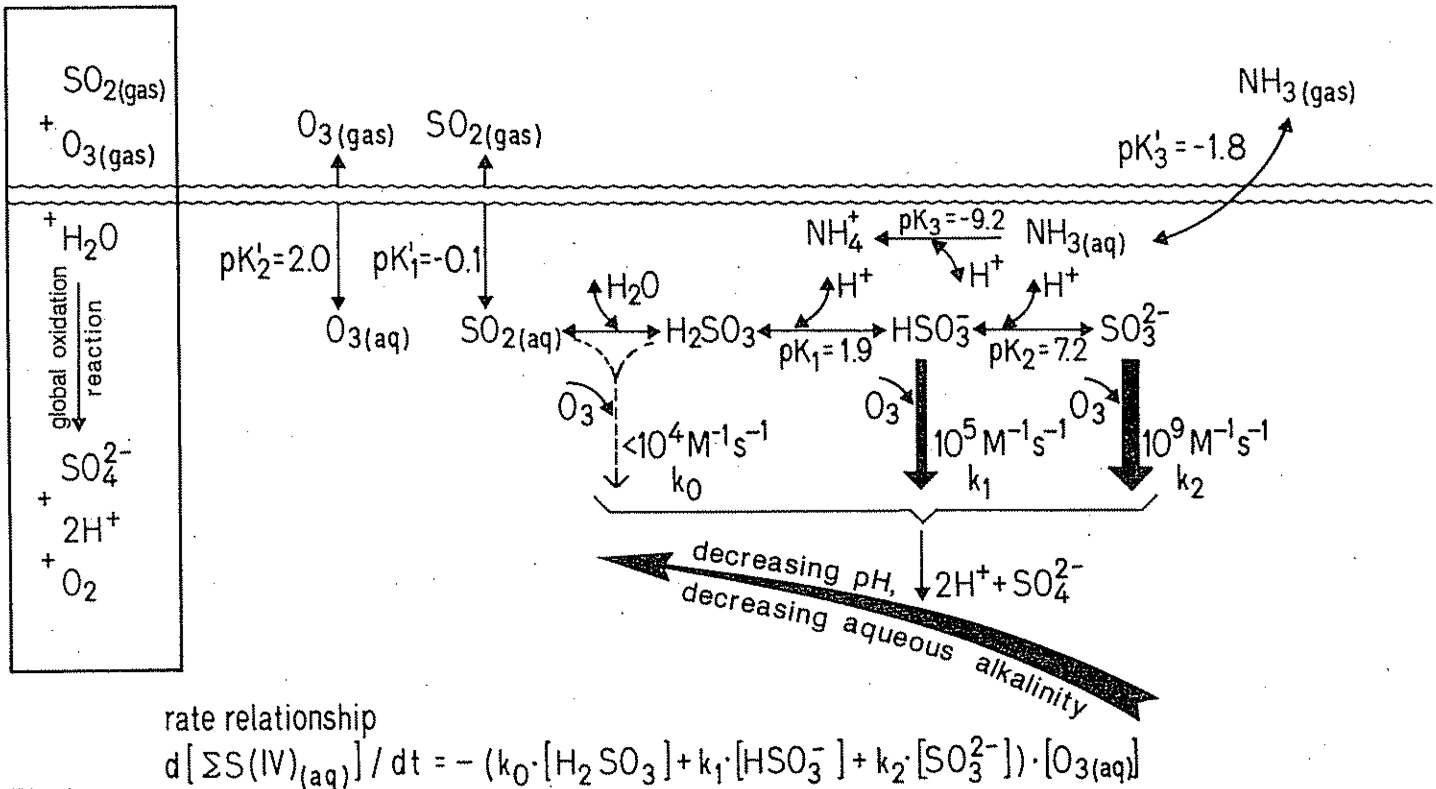

Fig. 1:
Pictorial representation of processes occuring in the aqueous phase: oxidation of SO_2 species by O_3 in the presence of NH_3; the rate constants are from [13] (after [11]). For every time increment, some of the H_2SO_4 is formed; the H^+ ions produced titrate the gas-water system along the "titration curve" to a slightly lower pH, and the aqueous alkalinity decreases.

recorded in Dübendorf, a suburb of Zurich, Switzerland. Of particular interest to us were the observations made during an accidental release of a few kg ammonia within 500 m of our sampling station and during a similar NH_3-experiment on purpose. The measurements of the fog composition showed in these studied cases that the variation of the concentration of SO_4^{2-} "followed" the variation of the NH_4^+ concentrations [6]. These data lend support to the simple hypothesis that NH_3 mediates the oxidation of SO_2 because

(1) the absorption of SO_2 into water is enhanced by an increase in pH;
(2) the oxidation of aqueous SO_2 increases with increasing pH:
(3) the buffering intensity provided by the NH_3 in the water and especially in the gas phase mitigates the lowering of the pH and thus in turn assists in sustaining relatively high oxidation rates; and
(4) the atmospheric acid neutralizing capacity (ANC), *i.e.* the alkalinity of the gas, aerosol and water phases together, ultimately determines the extent of SO_2 oxidation and the NH_4^+ to SO_4^{2-} ratio in the deposition.

The objective of this paper is to describe a model on the NH_3-mediated oxidation of SO_2 in aqueous phase by ozone, and to illustrate and discuss the applicability of the model to selected case studies.

- First, the chemical model is described; the acid-base neutralization process in the atmospheric system, gas-aerosol-water phases, are considered, and the concept of alkalinity is investigated for a gas-water system.
- Secondly, the evolution of the system with time is studied with regard to the alkalinity of the system, particularly the aqueous phase alkalinity. The role in the rate of the SO_2 oxidation of the addition of strong acid or aerosols into the system, as well as the variation of the liquid water content, is investigated.
- Finally, results from fog samples and from computations with this model are compared in order to improve the model, and to explain the fact that the NH_4^+, SO_4^{2-} and NO_3^- concentrations are in relatively constant proportions in the fog water droplets [6].

2. CHEMICAL MODEL

The oxidation of the SO_2 to SO_4^{2-} by dissolved H_2O_2, O_3, or by dissolved O_2 catalyzed by Fe(III), or Mn(II) in water is accompanied by the release of two protons [2]. In addition to the H_2SO_4 generated, various other strong acids (HCl, HNO_3, HNO_2) and bases (NH_3, alkaline dust containing $CaCO_3$, fly ash) are present in the atmosphere [5, 8]. The rate of oxidation of SO_2 in water depends on the oxidant, on solution variables, and on the presence of catalysts.

Our model system is built up by mixing various gases (CO_2, NH_3, SO_2, oxidant), and liquid water (water droplets), within a given volume, in a *closed* or *open* system. Also, acids (HCl, HNO_3) and bases (alkalinity from dust) can be added to the system. Then, a typical reaction sequence is established by oxidizing SO_2; the H^+ ions produced as a consequence of this oxidation "titrate" the gas-water system to a lower pH (fig. 1). In this model, O_3 is selected as the oxidant for SO_2. The rate expressions are characterized by a pH-dependence that is in accordance with the observations [5, 6], while oxidation with H_2O_2 is not.

For urban conditions and in winter time, it is reasonable to assume that the partial pressure of H_2O_2, p_{H2O2}, is lower than p_{O3} but also lower than p_{SO2}.

The NO_x oxidation in the aqueous phase is not considered.

At initial time, water droplets are assumed to condense in a given volume containing various atmospheric gases.

The extent of water droplet formation is assumed to be instantaneous, and is reflected in the liquid water content. Instantaneous (acid-base and gas-water) equilibrium and dissolution of aerosols in water are assumed. Mass transport to the droplet surface or mass transfer into the bulk phase is not considered as limiting [9], and is not taken into account.

2.1. CHEMICAL EQUILIBRIUM MODEL

Water, aerosol, and gas phases are taken into account in the chemical equilibrium model. Equilibria in our model system are characterized by Henry's law for exchanges between the gaseous and aquous phases and by acid-base equilibria in the aqueous phase.

(1) In the *open* system model, constant partial pressure of each gas component, (p_{SO2}) and (p_{NH3}), is maintained. The total mol balances for the sum of S(IV), and for the NH_3 species in water (fig. 1) are given by (see fig. 1 for the K-values):

$$\Sigma\,[S(IV)_{(aq)}] = (p_{SO2}) \bullet (K_1 + K_1' \bullet K_1 \bullet [H^+]^{-1} + K_1' \bullet K_1 \bullet K_2 \bullet [H^+]^{-2}) \qquad (1)$$

$$[NH_{3(aq)}]_T = [NH_{3(aq)}] + [NH_4^+] = (p_{NH3}) \bullet (K_3' + K_3' \bullet K_3^{-1} \bullet [H^+]) \qquad (2)$$

(2) In the *closed* system model, there is no exchange of matter between the considered volume of the system and the outside. Thus, the sum of component concentration in the gas and water phases within the total system remains constant. For the component C, this sum can be characterized by an initial partial pressure noted $(p_C)_0$, which is assumed for volume of the atmosphere before water droplets condense. If R is the gas constant, T the temperature, $\{C\}_T$ the total concentration in the gas-water system (in mol m^{-3}), C_i the concentration of the species i , in presence of liquid water in the atmosphere (q, in $l\ m^{-3}$), we can write for a component C:

$$\{C\}_T = (p_C)_0 / RT = (p_C) / RT + q \cdot \Sigma\,[C_{i,(aq)}] \qquad (3)$$

The distribution of NH_3 and SO_2 between the gas and water phases depends on pH, and, in a closed system, on the liquid water content. If $q = 10^{-4}\ l\ m^{-3}$, below pH 5.5, nearly all the NH_3 dissolves in water to form NH_4^+, while SO_2 is predominantly gaseous; above pH 8, NH_3 is mainly in the gas phase, and nearly all the SO_2 dissolves to form SO_3^{2-}-ions.

2.2 ATMOSPHERIC ACIDITY AND ALKALINITY

It is essential to consider the acid-base neutralization process in the ***entire*** atmospheric system. The concept of atmospheric acidity and alkalinity was introduced to interpret the interactions of NH_3 with strong acids emitted into and/or produced within the atmosphere [8, 10]. A net atmospheric acidity can be defined by summing over all ***potential*** acids and bases in the gas, aerosol and liquid phases, using reference conditions for specific redox conditions, and assuming the presence of liquid water. Alkalinity is defined by a net proton balance with regard to a reference level; that is the sum of the concentrations of all the species containing protons in deficiency minus the concentrations of the species containing protons in excess of the proton reference level.

The emission of gaseous NH_3 into the atmosphere essentially "titrates" the inputs of the potential strong acids. In case of a residual atmospheric alkalinity, all the SO_2 absorbed into a water droplet will be relatively readily converted into H_2SO_4. On the other hand, in case of residual atmospheric acidity, *i.e.* the ammonia cannot "neutralize" the acids present and the acidity generated by SO_2 oxidation, SO_2 oxidation by O_3 becomes kinetically delayed (*autoinhibition due to the lowering of the pH as a consequence of SO_2 oxidation*). The ammonia - by influencing pH, buffer intensity and ANC - essentially regulates the extent of SO_2 oxidation by O_3. The oxidation starts instantaneously, *i.e.* as soon as the pH is sufficient high, and occurs within a time period of a few hours. Thus, we can expect in atmospheric water droplets (cloud, liquid aerosol , rain,) relatively constant proportion of NH_4^+ to SO_4^{2-} ($[NH_4^+] / [SO_4^{2-}] \approx 2$).

If NH_3 and SO_2 are in an open system, the buffer intensity is very high and the pH variation is not large: gaseous NH_3 is able to neutralize the acid additions by forming NH_4^+, while SO_2 can neutralize the base additions.

If NH_3 and SO_2 are in a closed system, the buffer intensity is significant as long as all NH_3 is not exhausted in gas phase, and is able to be dissolved into water to neutralize acid addition.

On the other hand, in a *homogeneous* and closed system in which NH_3 and SO_2 are considered as being non-volatile, the pH-range is very large: the buffer intensity is very low if some acid is added.

A new computer program is being built up [11] using the chemical equilibrium program, MICROQL [12]. Alkalimetric and acidimetric titration curves can be calculated using electroneutrality equation or proton condition. The variables are the initial partial pressures of SO_2, NH_3, and O_3, the liquid water content, the aerosol concentrations, and the concentrations of base (alkaline dust, *e.g.* $CaCO_3$) or strong acid (HNO_3, HCl, or H_2SO_4).

3. RESULTS AND DISCUSSION

3.1. DYNAMIC BEHAVIOUR OF SOLUTIONS WITH SO_2 OXIDATION IN AQUEOUS PHASE

In order to illustrate the results of our computer simulations, we will first consider the simplified system CO_2, NH_3, SO_2, O_3, and H_2O. Two cases are exemplified in fig. 2:

(a) $(p_{NH3})_0 < 2(p_{SO2})_0$
(b) $(p_{NH3})_0 > 2(p_{SO2})_0$.

In both cases, the system is open with respect to CO_2 and O_3. For every time increment, some of the H_2SO_4 is formed and the H^+ ions produced titrate the gas-water system along the "titration curve" to a slightly lower pH. An initial rapid decrease in pH (concordant with an increase in SO_4^{2-} and NH_4^+ concentrations) is followed by an asymptotic approach to a steady state value(fig. 2a, b).

Case a: low NH_3 partial pressure $(p_{NH3})_0 < 2(p_{SO2})_0$

At the conclusion of the simulation, the SO_4^{2-} concentration and pH are low; nearly all the NH_3 dissolves to form NH_4^+. Since $[NH_4^+]/[NH_3]_0$ is close to 1, the ANC of NH_3 becomes rapidly exhausted; most of the NH_3 in the system will be in the water phase as NH_4^+ (fig. 2c). The pH being too low, the oxidation of SO_2 is very slow. The ratio $[NH_4^+]$ to $[SO_4^{2-}]$ approaches 2 within a few hours. But at the end of the simulation, SO_4^{2-} is still being produced at a

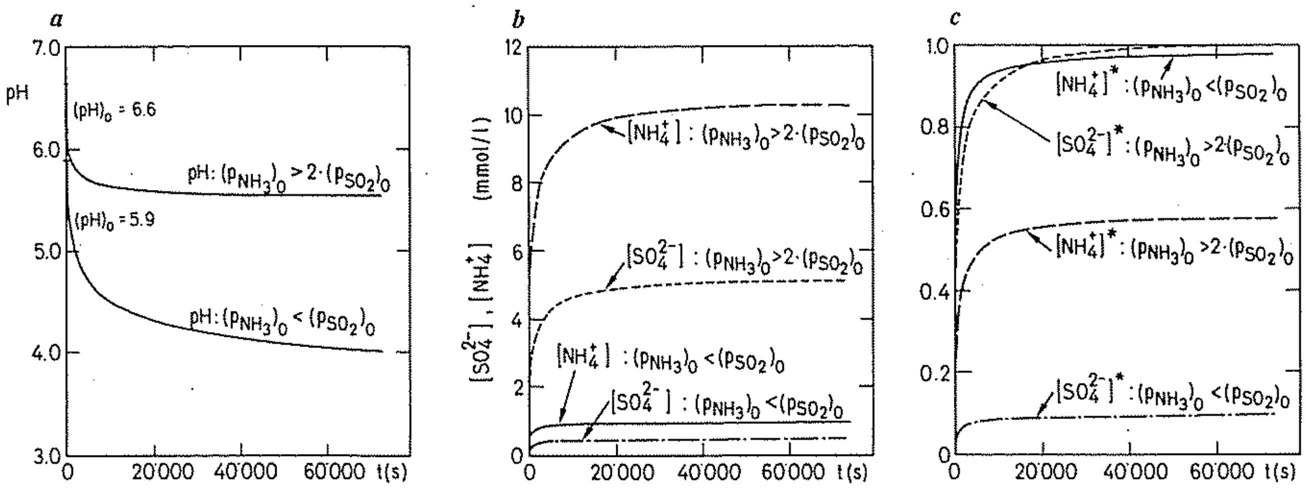

Fig. 2:

Variation in aqueous phase composition as a consequence of SO_2 oxidation: $[NH_4^+]$ and $[SO_4^{2-}]$, pH, $[NH_4^+]^*$ and $[SO_4^{2-}]^*$ vs. time. (a) ***Low NH_3 partial pressure $(p_{NH3})_0 < 2\,(p_{SO2})_0$ with $(p_{NH3})_0 = 4.3\ 10^{-9}$ atm ($[NH_3]_0 = 9.6\ 10^{-4}$ mol l^{-1});*** (b) ***NH_3 in relative excess $(p_{NH3})_0 > 2(p_{SO2})_0$ with $(p_{NH3})_0 = 8.0\ 10^{-8}$ atm ($[NH_3]_0 = 1.8\ 10^{-2}$ mol l^{-1})***
Initial conditions: $(p_{SO2})_0 = 2.3\ 10^{-8}$ atm ($[SO_2]_0 = 5.1\ 10^{-3}$ mol l^{-1}); $[NH_4NO_3]_{aerosol} = 1.0\ 10^{-8}$ mol m^{-3} ($[NO_3^-] = 5.5\ 10^{-4}$ mol l^{-1}); $(p_{O3})_0 = 1.5\ 10^{-8}$ atm; $(p_{CO2})_0 = 10^{-3.5}$ atm; $q = 1.84\ 10^{-4}$ l m^{-3}; NH_3 and SO_2 are in closed system; O_3 and CO_2 are in open system. N.B.: ***$[NH_4^+]^* = [NH_4^+]/[NH_3]_0$ and $[SO_4^{2-}]^* = [SO_4^{2-}]/[SO_2]_0$***

very low rate. In this case, the consumption of SO_2 is small (less than 10 %), and its influence on the rate of oxidation is not significant: the system becomes as if it was open with regard to SO_2 ($p_{SO2} \approx$ constant).

Case b: NH_3 in relative excess $(p_{NH3})_0 > 2(p_{SO2})_0$

Although SO_4^{2-} production is extensive, the excess of NH_3 (mostly in the gas phase) is sufficient to maintain the pH at a higher value than in the previous case, and the oxidation becomes very fast (fig. 2a, b). The drop in pH comes to an end as soon as SO_2 becomes exhausted (fig. 2a, c). Then, the ratio $[NH_4^+]$ to $[SO_4^{2-}]$ is 2 and constant with time. But, NH_3 is not in sufficient excess for the system to be considered as an open one: an important part of it is used to neutralize the H^+ ions formed by the oxidation to SO_4^{2-}.

The ideas presented here for simple NH_3, SO_2, O_3, CO_2, and H_2O systems are readily extended to more complex situations. The addition of other strong acids (like HNO_3 or HCl) or strong bases (such as CaO from fly ash) has as a consequence the shift of the gas-water system along the titration curve.

3.2. ADDITION OF NEUTRAL AEROSOLS

Our simulation model considers the uptake of aerosols into the water droplets by adjusting the electroneutrality equation. It is interesting to note that the addition of a "neutral" aerosol (*e.g.* following a relationships $[NH_4^+] = 2[SO_4^{2-}] + [NO_3^-]$) may change the alkalinity of the water droplets because the partitioning of the alkalinity between the gas phase and the water phase (due to NH_3 distribution) may become changed; in other words, the uptake of "neutral" aerosols may reduce the alkalinity of the water phase, and in turn decrease the rate of SO_2 oxidation, because some of the aerosol NH_4^+ ends up as NH_3 in the gas phase.

3.3. EFFECT OF LIQUID WATER CONTENT

The titration curve for a closed system and for given initial conditions in a closed system is a function of the ratio volume of water to volume of system, *i.e.* the liquid water content, q, and pH. From this point of view, the consequence of an increase of q (isothermal condensation) is a modification of the distribution of NH_3 between the gas and water phases. When q is very large, the conditions tend to the homogeneous system, the gaseous phase being negligible. On the contrary, if q is small, the gaseous phase can be considered as a large reservoir for the water soluble species, specially for NH_3. This illustrates how important it is to measure reliably the water content during a fog event because it affects all solution variables.

3.4. COMPARISON OF FIELD DATA OF FOG EVENT WITH KINETIC CALCULATIONS

The simulation of a fog event requires the knowledge of input variables such as the concentrations of the gas phase, the concentrations of aerosols, the composition of condensation nuclei, and the evolution of the liquid water content, of the gas phase content and of the temperature with time. The comparison of simulation data with the experimental results observed during a fog event is a valuable test and may help to improve the model. We selected two fog events, an acid fog and a "neutral" fog (pH = 7), for this comparison. The composition of these fogs and its variations with time were described earlier [6]. Before and during the two fog events, both gas phase SO_2 and O_3 are measured near the sampling site [personal communication by R. Gehrig, EMPA, Dübendorf, 1988; see captions of fig. 3 and 4]. For our model calculations, we used as input data the composition of the gases (NH_3, HCl, HNO_3) and the liquid water content. The system is assumed to be open with respect to O_3 and CO_2.

It was observed in our investigations on fog events that the NH_4^+ concentration is often approximately equal to the equivalent sum of the NO_3^- and SO_4^{2-} concentrations. Moreover, the ratios $[NH_4^+] / [SO_4^{2-}]$ and $[NH_4^+] / [NO_3^-]$ are constant and equal to 3.6 and 1.9 (in mol/mol) respectively. Two possible explanations were proposed [6]: (1) after its absorption in the water droplets, the gas phase SO_2 is oxidized to SO_4^{2-} in proportion to the available NH_3; (2) the NH_4^+, SO_4^{2-}, and NO_3^- concentrations are in relatively constant proportions in aerosols of approximate composition $\{(NH_4)_2SO_4 \cdot 2\,NH_4NO_3\}$, *i.e.* SO_2 oxidation and neutralization occurred in the aerosols, prior to their becoming dissolved in the fogwater droplets. The aerosols provide a substantial fraction of these components in the fogwater.

a) Acid fog
Advection of HCl, from stack gases of a refuse incineration plant located *ca.* 3 km from the sampling point, affected the pH and the composition of the fog. The larger the pulses of HCl, the lower the pH: at low pH values, the concentration of protons is nearly equal to the Cl^- concentration, *i.e.* HCl is regulating the pH. For calculations, we assumed a system closed with respect to NH_3 and SO_2. The two parameters that had the greatest effect on the composition and temporal variation in the fog composition were (1) HCl that regulates H^+ concentration and coinciding with Cl^- concentration (fig. 3a); and (2) the liquid water content, *i.e.* the density of the fog, whose variations with time essentially determined the variations in the concentrations of ions, present in constant proportions (fig. 3b).
In order to obtain a good agreement between the results of the field data and the computed model data, an incipient concentration of SO_4^{2-} equal to 1.7 10^{-4} mol l^{-1} had to be implied. This means that, primarily because of low pH, relatively little SO_2 became oxidized subsequent to the fog formation.
The results of the simulation indicate that the low pH of the water droplets precluded the oxidation of the SO_2; thus the conditions before the formation of the fog, especially the compositions of the aerosols, that were then taken up by the water droplets, determine the proportions of the different components in the fogwater, particularly the NH_4^+, SO_4^{2-}, and NO_3^- concentrations

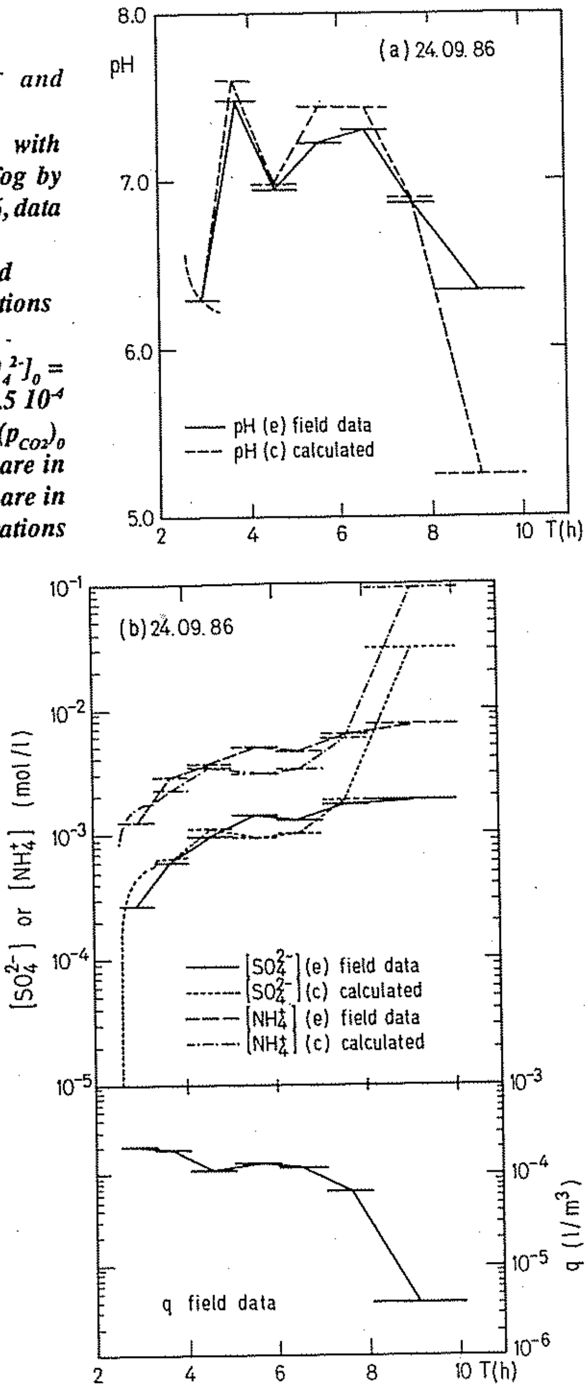

Fig. 3
a) pH vs time and
b) SO_4^{2-} or NH_4^+ and q vs. time:
Comparison of field data with kinetic calculations: acid fog by absorption of HCl (22.09.86, data after [6])
(e): measured field data and
(c): results of the computations
Initial conditions:
$(p_{SO_2})_0 = 4.2\ 10^{-9}$ atm; $[SO_4^{2-}]_0 = 1.7\ 10^{-4}$ mol l^{-1}; $[NO_3^-]_0 = 3.5\ 10^{-4}$ mol l^{-1}; $(p_{O_3})_0 = 5.1\ 10^{-9}$ atm; $(p_{CO_2})_0 = 10^{-3.5}$ atm; NH_3 and SO_2 are in closed system; O_3 and CO_2 are in open system. The concentrations of NH_3, HCl, HNO_3 and the liquid water content used in the program varied during the simulation as they varied during the fog event.

b) "Neutral fog"
This "experiment" is particularly interesting as it demonstrates the mediating role of NH_3. Indeed, because of the continued release of gas phase NH_3, the excess of NH_3 was sufficient to maintain the pH close to 7. We were justified in assuming that the partial pressure of NH_3 is nearly constant over the entire duration of the fog. The results presented in fig. 4 are obtained with the assumption that the system is closed with respect to SO_2, and the initial concentration of SO_4^{2-} is equal to 0. In this case, all the SO_2 is exhausted by oxidation by O_3, and transformed into SO_4^{2-}. The agreement between field data and computed results is good for pH, NH_4^+, and SO_4^{2-}: we can simulate the variations of the concentrations with time. Contrary to the previous case, *i.e.* acid fog, we obtain the expected values for the ratio $[NH_4^+]/[SO_4^{2-}]$ by assuming that all the SO_4^{2-} is due to the oxidation of the SO_2 present at time 0. Two conditions have to be combined: a sufficient amount of SO_2 and a quite high pH (>6). The first assumption [6] is in accord with the constant ratios observed in this "neutral" fog. As in the previous case, the role of the liquid water content is evident. When the fog disappears at 8.00 p.m., *i.e.* q decreases, a discrepancy between field data and calculated concentrations (fig. 3 and 4) is probably due to the difficulties in measuring q and in sampling fogwater during fog dissipation.

4. CONCLUSIONS

A model on the oxidation of SO_2 by O_3 in atmospheric aqueous phase (fog, cloud, rain water) shows that ammonia plays a fundamental role in neutralizing the acidity produced by the strongly pH-dependent oxidation of SO_2; the amount of available ammonia and its partition between the gaseous and aqueous phases (depending on the pH of the aqueous phase, and in a closed system on the liquid water content) regulates the alkalinity of the aqueous phase, and in turn drives the production of SO_4^{2-}. If in the initial air volume SO_2 is present in excess with respect to ammonia, the production of SO_4^{2-} will be limited by acidification of the aqueous phase after exhaustion of the ANC of NH_3; if on the contrary NH_3 is present in excess, the production of SO_4^{2-} is very effective and

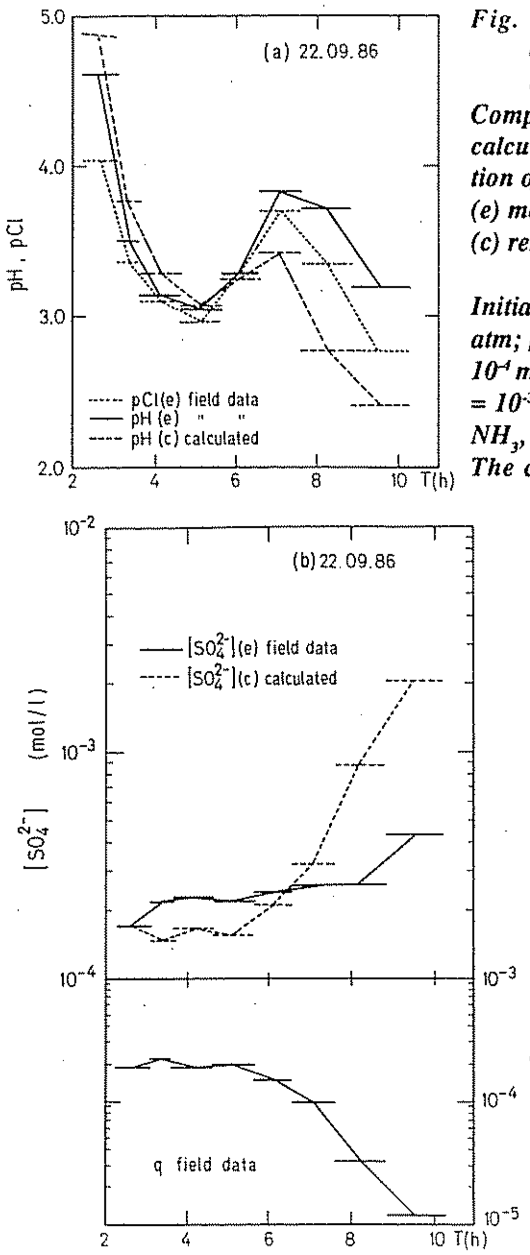

Fig. 4
a) pH, pCl vs time and
b) SO_4^{2-} and q vs. time:
Comparison of field data with kinetic calculations: "neutral" fog by absorption of NH_3 (24.09.86, data after [6]); (e) measured field data and (c) results of the computations

Initial conditions: $(p_{SO2})_0 = 3.1\ 10^{-9}$ atm; $[SO_4^{2-}]_0 = 0$ mol l^{-1}; $[NO_3^-]_0 = 4.8\ 10^{-4}$ mol l^{-1}; $(p_{O3})_0 = 4.0\ 10^{-9}$ atm; $(p_{CO2})_0 = 10^{-3.5}$ atm; SO_2 is in closed system; NH_3, O_3 and CO_2 are in open system. The concentrations of Cl^-, NH_3, and the liquid water content used in the program varied during the simulation as they varied during the fog event

may exhaust the available SO_2.

The presence of other acid gases (HCl, HNO_3, etc), of "neutral" aerosols components ($(NH_4)_2SO_4$, NH_4NO_3, etc), and of basic components ($CaCO_3$) affects the pH of the aqueous phase and the dissolution equilibria of NH_3 and SO_2, and influences thus the production of sulfate from SO_2. The comparison of field measurements on the composition of radiation fogs with model computations supports the reaction sequence postulated.

During the fog events, new components enriched with SO_4^{2-}, either H_2SO_4 or $(NH_4)_2SO_4$ [7], are formed. Water droplets are considered as chemical reactors for the SO_2 oxidation as well as vectors for the component transport. They can be intercepted by vegetation canopies; the substances become more concentrated by evaporation, and react with needles or leaves. On the other hand, the deposition of acid and sulfate-bearing fog on soils and into surface waters can cause an acidification of these media, and in turn can cause weathering, remobilization of metals or nutrients for plants.

ACKNOWLEDGEMENT: Appreciation is expressed to Mrs. H. Bolliger for drawing the pictures. This research was supported by Schweizerischer Nationalfond (National Programme on Air Resources NFP-14).

[1] Jacob D.J. and Hoffmann M.R., A dynamical model for the production of H^+, NO_3^-, and SO_4^{2-} in urban fog. J. geophys. Res., (1983) 88, 6611-6621.

[2] Seinfeld J.H., Atmospheric Chemistry and Physics of Air Pollution. Wiley, New York, (1986).

[3] Munger J.W., Jacob D.J., Waldman J.M. and Hoffmann M.R., Fogwater chemistry in an urban atmosphere. J. geophys. Res., (1983) 88, 5109-5121.

[4] Zürcher F. and Gisler B., Beitrag von Ammonium zur nassen Deposition von Schwefelverbindungen. Proc. 4th Europ. Sympos. on Physico-Chemical Behaviour of Atmospheric Pollutants (edited by Angeletti G., Restelli G.). D. Reidel Publ. Co., Dordrecht, (1987) pp. 480-488.

[5] Johnson C.A., Sigg L. and Zobrist J., Case studies on the chemical composition of fogwater: the influence of local gaseous emissions. Atmospheric Environment, (1987) 21, 2365-2374.

[6] Sigg L., Stumm W., Zobrist J. and Zürcher F., The chemistry of fog: factors regulating its composition. Chimia, (1987) 41, 159-165.

[7] Ruprecht H. and Sigg L., Interactions of aerosols (ammonium sulfate, ammonium nitrate and ammonium chloride) and of gases (HCl, HNO_3) with fogwater. Submitted to Atmospheric Environment.

[8] Jacob D.J., Munger J.W., Waldman J.M. and Hoffmann M.R., The H_2SO_4-HNO_3-NH_3 system at high humidities and in fogs: I. Spatial and temporal patterns in the San Joaquin Valley of California. J. geophys. Res., (1986) 91, 1073-1088.

[9] Schwartz S.E. and Freiberg J.E. Mass-transport limitation to the rate of reaction of gases in liquid droplets: application to oxidation of SO_2 in aqueous solutions. Atmospheric Environment, (1981) 15, 1129-1144.

[10] Liljestrand H.M., Average rainwater pH, concepts of atmospheric acidity, and buffering in open systems. Atmospheric Environment, (1985) 19, 487-499.

[11] Behra Ph., Sigg L. and Stumm W., Dominating influence of NH_3 on the oxidation of aqueous SO_2: The coupling of NH_3 and SO_2 in atmospheric deposition. Submitted to Atmospheric Environment.

[12] Westall J., MICROQL - I: A chemical equilibrium program in BASIC. Report, EAWAG, Dübendorf (CH), (1979).

[13] Hoigné J., Bader H., Haag W.R. and Staehelin J., Rate constants of reactions of ozone with organic and inorganic compounds in water - III Inorganic compounds and radicals. Water Res., (1985) 19, 993-1004.

Philippe Behra has studied rural civil engineering in France. He got his PhD. for a thesis on the transport of trace metals in groundwater at the Louis Pasteur University of Strasbourg. At EAWAG he works on the project on atmospheric depositions, running under the context of a national program.

KINETICS OF DISSOLUTION OF FE(III)(HYDR)OXIDES IN NATURAL WATERS

BARBARA SULZBERGER, DANIEL SUTER, CHRISTOPHE SIFFERT, STEVEN BANWART, AND WERNER STUMM

The cycling of iron in natural environments is of great importance to the biogeochemical cycling of other reactive elements such as heavy metals and nutritients. Iron(III) usually occurs as relatively insoluble iron(III)(hydr)oxide while the lower oxidation state is more soluble. The principal phases observed in natural waters and sediments are hematite (α-Fe_2O_3), goethite (α-FeOOH), lepidocrocite (γ-FeOOH), maghemite (γ-Fe_2O_3), magnetite (Fe_3O_4), and ferrihydrite ($Fe_2O_3 \cdot nH_2O$). The latter phase is a group name for X-ray amorphous Fe^{III} phases with rather high specific surface areas (up to a few hundred m^2g^{-1}). This amorphous phase is in natural waters a rather widespread authigenic form that may originate from mononuclear $Fe^{III}(OH)_i^{(3-i)-}$, formed from oxygenation of Fe^{II} and subsequent hydrolysis. The ferrihydrite is transformed in sediments into the thermodynamically more stable α-FeOOH and α-Fe_2O_3 [1].

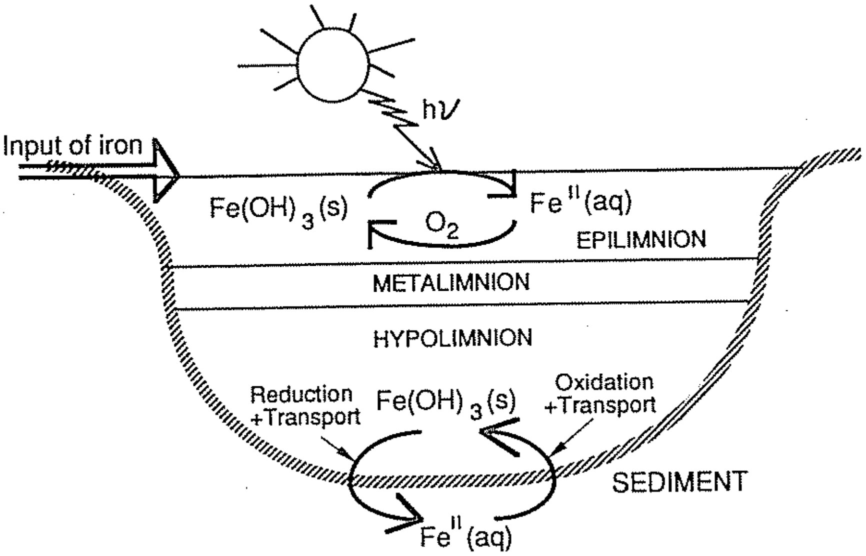

Fig. 1.
Transformation of iron in a lake during the summer stagnation period.

The redox cycles of iron in a surface water is schematically depicted in fig. 1. Thermodynamically, the redox process occuring at an oxic-anoxic boundary may be represented by the reaction:

$$Fe^{2+}(aq) + 3\,H_2O \leftrightarrows Fe(OH)_3(s) + 3\,H^+ + e^- \tag{1}$$

which has a redox potential around 0 volts ($p\varepsilon \cong 0$) for the conditions encountered in surface waters (pH = 7-8). The reduction of iron is thus accompanied by dissolution and the oxidation by precipitation. Usually, dissolved oxygen is the oxidant of Fe^{II}; the rate of oxidation as a function of pH and other solution variables is well known [2-3]. Organic solutes and S^{-II} compounds, resulting from the decompositon of biological material or from exudates of organisms are the reductants of the insoluble Fe^{III} phases. All organic solutes are, thermodynamically speaking, reductants of Fe^{III}. However, many organic solutes are metastable with regard to Fe^{III}; i.e. they do not undergo redox reactions spontaneously unless catalyzed by light. Hence, the reaction

$$Fe(OH)_3(s) + \text{organic solutes} \leftrightarrows Fe^{II} + \text{oxidized organic solutes} \tag{2}$$

is often enhanced by light.Thus, in the light-accessible part of oxic epilimnetic water a steady state concentration of dissolved iron(II) is maintained through photochemical processes[4-5].The light-induced reductive dissolution may be of considerable importance in the release of bioavailable Fe^{II} to organisms in surface waters [5].

The redox cycles of iron, which are accompanied by dissolution and precipitation, are coupled to the cycle of other reactive compounds, since the oxidation of iron(II) to iron(III)(hydr)oxide is accompanied by the binding of reactive compounds, such as heavy metals, metalloids and phosphates to the iron(III)-(hydr)oxide surface, and the reduction of iron(III)(hydr)oxides to dissolved iron(II) is accompanied by the release of these compounds into the water.

The cycling of iron also plays an important role in soil systems, particularly in the formation of podsoils under the influence of acid deposition. The chemistry of the formation and dissolution of iron(III)(hydr)oxides is also of importance in corrosion and its inhibition.

THEORETICAL BACKGROUND

At the surface of hydrous oxides, functional OH-groups are able to interact with H^+ ions, metal ions and ligands [6]. Ligands become bound to the Fe^{III} centers at the surface of the hydrous oxide, which act as Lewis acids. In a relatively fast ligand exchange reaction surface OH-ions are replaced, e.g., by the anion of a dicarboxylic acid like oxalate. Thereby inner-sphere surface complexes can be formed. The reactivity of iron-(III)(hydr)oxides, e.g. towards dissolution, critically depends upon the structure of the surface complex. It has been shown, that ligands, which are able to form chelate complexes at the surface of a hydrous iron(III) oxide, are especially efficient in promoting the dissolution of the hydrous oxide [7]. The dissolution kinetics of iron(III)(hydr)-oxides is controlled by surface processes and not by transport processes.

The various pathways for the dissolution of iron(III)(hydr)oxides are schematically shown in fig. 2. The structures given in this figure are highly schematic, they are not intended to give the details on the structural or coordinative arrangements; they illustrate the presence of surface hydroxo groups and of oxo- and hydroxo-bridges. This schematic presentation illustrates the type of reactions that can occur and that steady state mechanisms are possible as the

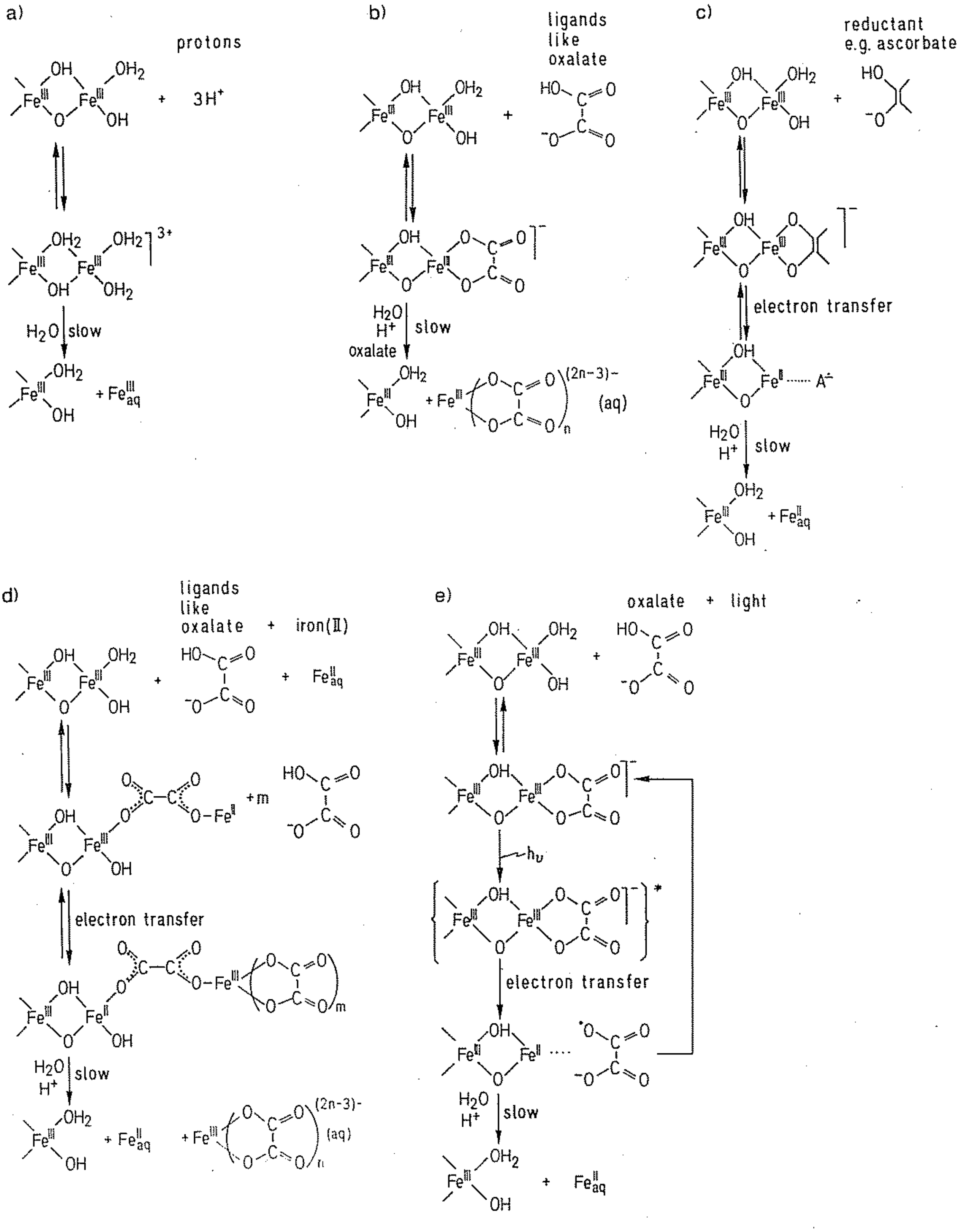

Fig. 2.
Schematic representation of the various reaction modes for the dissolution of iron(III)(hydr)oxides:
a) by protons;
b) by bidentate complex formers that form surface chelates;
c) by reductants such as ascorbate that can form surface complexes and transfer electrons inner-spherically;
d) catalytic dissolution of iron(III)(hydr)oxides by Fe^{II} in the presence of a complex former;
e) light-induced dissolution of iron(III)(hydr)oxides in the presence of an electron donor such as oxalate.

original surface structure is restored after detachment of the surface groups. The first two pathways a) and b) show, respectively, the influence of H$^+$ and of surface complex-forming ligands. The binding of H$^+$ and/or of ligands by the surface results in the weakening of the bonds in the proximity of a surface Fe^{III} center followed by detachment of this center from the surface and release

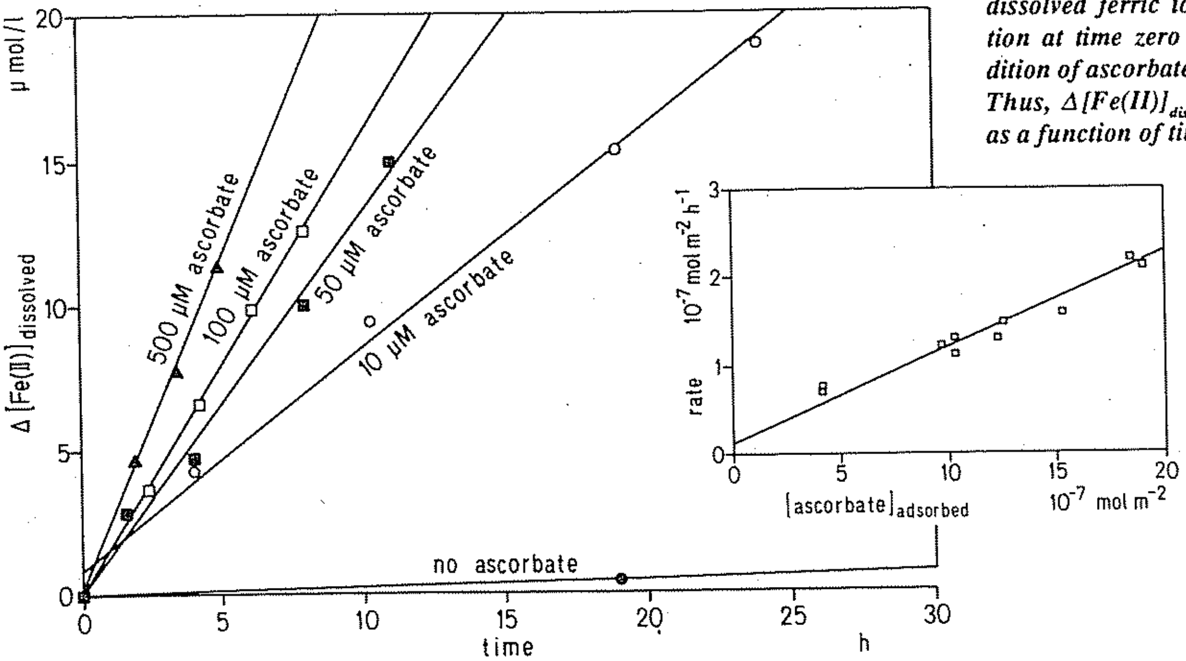

Fig. 3.
Reductive dissolution of hematite at pH 3 in the presence of ascorbate as the reductant:
The different ascorbate concentrations correspond to initial concentrations. The suspension contained 0.5 g/l hematite. The dissolved ferric ion concentration at time zero after the addition of ascorbate is set to zero. Thus, $\Delta[Fe(II)]_{dissolved}$ is shown as a function of time.

into solution. The detachment step is generally rate determining for the whole process.

A reductant can readily exchange electrons with an Fe^{III} surface center if it is specifically adsorbed to the hydrous oxide surface. Especially efficient are those reductants that form inner-sphere surface complexes such as e.g. ascorbate (fig. 2c). The electron transfer leads to an oxidized reactant (which is often a radical) and to a surface Fe^{II} ion. The latter is - because of the larger lability of the Fe^{II}-O-bond in the crystalline lattice surface compared to the corresponding Fe^{III}-O-bond - more easily detached from the surface than a Fe^{III} center. We assume that also in reductive dissolution of iron(III)(hydr)oxides the detachment is the rate determining step.

In the presence of metastable ligands that form surface complexes with Fe^{III} of a hydrous oxide, i.e. oxalate, reductive dissolution of iron(III)(hydr)oxides - although thermodynamically favourable - does not occur unless induced by light. This is depicted in fig. 2e. Here, an electronic excited state, indicated with a star, is involved in the redox-process. Either the surface complex or the iron(III)(hydr)oxide itself may act as the light-absorber and charge transfer may occur from an electronic excited state of the surface complex or of the iron(III)(hydr)oxide bulk phase [8].

In the reaction mode shown in fig. 2d iron(II) is the reductant for the reductive dissolution of iron(III)(hydr)oxides. Fe^{2+}, however, does not to a measurable extent exchange electrons with peripheral iron(III) of an iron(III)(hydr)oxide in the absence of a complex former. Such an electron transfer, however, can occur in the presence of a suitable ligand, e.g., oxalate, which can act as a brigding ligand. As illustrated in fig. 2d, a ternary surface complex is formed and an inner-sphere electron transfer takes place from the adsorbed iron(II) to the surface iron(III), followed by the detachment as the rate determining step. $Fe^{II}(aq)$ acts as a catalyst for the dissolution of iron(III)(hydr)oxides, since its concentration remains constant, while the concentration of dissolved iron(III) increases.

The various dissolution pathways can occur simultaneously, which must be considered in formulating rate laws; the overall rate law is often not just the sum of the individual ones.

RESULTS FROM LABORATORY EXPERIMENTS

Fig. 3 shows experimental results on the reductive dissolution of hematite in the presence of various concentrations of ascorbic acid at pH 3 [9]. The dissolution increases linearly with time at a given ascorbate concentration. The dissolution rate, R, is directly proportional to the concentration of adsorbed ascorbate, $\{>FeA^-\}$, (Fig. 3, insert):

$$R = k\{>FeA^-\} \qquad (3)$$

where

$$\{>FeA^-\} = \frac{S\,K^s\,[HA^-]}{1 + K^s\,[HA^-]} \qquad (4)$$

according to the following equilibrium of the surface complex formation:

$$>FeOH + HA^- \rightleftarrows\ >FeA^- + H_2O \qquad (5)$$

> is a short hand symbol for the binding of the surface iron center to the crystalline lattice of hematite, K^s is the equilibrium constant of the adsorption equilibrium, $[HA^-]$ is the concentration of ascorbic acid in solution and S [mol m^{-2}] the maximum capacity of the α-Fe_2O_3 surface for the adsorption of ascorbate, $S = \{>FeOH\} + \{FeA^-\}$.

Fig. 4 shows the dissolution of hematite as a function of time at different concentrations of iron(II) added to the suspension. Obviously, at a given oxalate concentration, the dissolution rate increases with increasing iron(II) concentration. The dissolution rate is again a Langmuir-type function of the concentration of dissolved iron(II) [10]. This Fe^{II}-effect may be explained by the formation of a ternary complex with Fe^{II} at the hematite surface in the presence of oxalate or other suitable ligands. We assume that electron transfer occurs through the ligand to the Fe^{III} at the surface, as shown in fig. 2d.

Fig. 5 shows the light-induced dissolu-

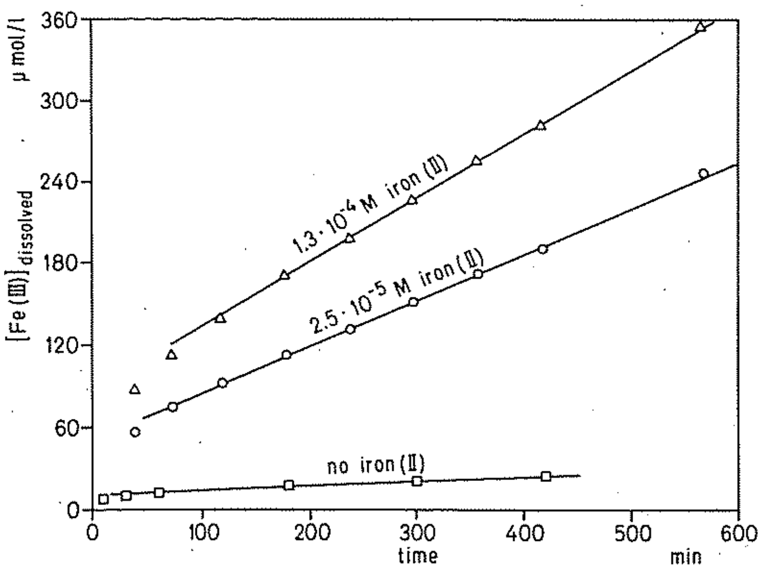

Fig. 4.

Fe^{II}-catalyzed dissolution of hematite in the presence of oxalate at pH 3. Total oxalate concentration: 3.3 mmol/l, 0.5 g/l hematite. The indicated concentrations correspond to the total concentration of added ferrous iron. Because of inhomogeneities at the hematite surface the initial dissolution is faster. The dissolution rates are determined from the linear part of the dissolution experiment.

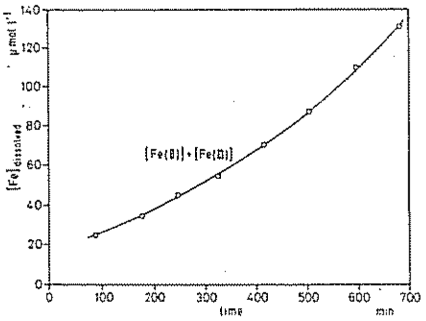

Fig. 5.

Light-induced dissolution of hematite at a relatively low light intensity: $I_o = 4$ W/m²; $\lambda = 375$ nm. Initial oxalate concentration: 3.3 mmol/l; 0.5 g/l hematite, pH = 3; nitrogen atmosphere; irradiated surface: $\cong 50$ cm²; reaction volume: 250 ml.

tion of hematite in the presence of oxalate [11]. Unlike in the dark, the rate of the light-induced dissolution of hematite is not constant but increases with time. This can be explained in terms of the superimposition of different reaction modes, in this case pathway d) and e). Under the influence of light a photoredox reaction occurs either at the surface of the hematite or in solution leading to formation of dissolved iron(II) and to the oxidized electron donor, which is in the case of oxalate CO_2. The surface photoredox process occurs according to the following stoichiometry:

$$\alpha\text{-}Fe_2O_3 + C_2O_4^{2-}(ads.) + 6\,H^+ \xrightarrow[N_2]{h\nu} 2\,Fe^{2+} + 2\,CO_2 + 3\,H_2O \qquad (6)$$

The photochemically formed dissolved Fe^{II} catalizes the dissolution in a thermal reaction whereby dissolved Fe^{III} is formed, as shown in fig. 4. Thus, in this case we are dealing with two coupled reactions which result in an **autocatalytic dissolution** of hematite. Such an autocatalytic dissolution has also been observed with goethite under the influence of light [12].

CONCLUSIONS

The most important conclusions from our laboratory experiments are enumerated below. An overwiev of our experimental work is given in [13].

1) Processes at the surface of iron(III)-(hydr)oxides and not transport processes control the dissolution kinetics.

2) The formation of **inner-sphere surface complexes** is involved in the dissolution of iron(III)(hydr)oxides.

3) The rate of dissolution is directly proportional to the surface concentration of the compound that is specifically adsorbed on the iron(III)(hydr)oxide surface.

4) During the dissolution process, the surface of the hydrous iron(III) oxide is, after detachment of the surface group, reconverted into its original configuration.

5) The dissolution of iron(III)(hydr)oxides can occur through different pathways, which can be superimposed, so that the rate of the overall dissolution process is often not just the sum of the individual rates.

From laboratory to field experiments

In order to become aware of some of the various factors that influence the dissolution of iron(III)(hydr)oxides in a natural environment, we must abstract from the complexity of nature and carry out simplified laboratory experiments with model systems, where we can control the variables. Many of our experiments have been carried out at low pH values and with crystalline iron(III)(hydr)oxide modifications such as hematite, because it is more convenient to assess the reaction mode with well defined surfaces. We have ascertained, however, that the reactions described usually also occur at higher pH-values, although the rates may then be lower. It is important now to evaluate the validity of the postulated rate laws from laboratory experiments for natural aquatic systems.

[1] U. Schwertmann and W.R. Fischer, Zur Bildung von a-FeOOH und a-Fe_2O_3 aus amorphem Eisen-(III)hydroxid, Z. Anorg. Allgem. Chem., (1966) *346*, 137.

[2] W. Stumm and F. Lee, Oxygenation of ferrous iron, Ind. Engin. Chem., (1961) *53*, 143.

[3] F.J. Millero, S. Sotolongo and M. Izaguirre, The oxidation kinetics of Fe(II) in seawater, Geochim. Cosmochim. Acta, (1987) *51*, 793.

[4] R.H. Colienne, Photoreduction of iron in the epilimnion of acidic lakes, Limnol. Oceanogr., (1983) 28, 83.

[5] T.D. Waite and F.M.M. Morel, Photoreductive dissolution of

loidal iron oxides in natural waters, Environ. Sci. Technol., (1984) *18*, 860.

[6] P.W. Schindler and W. Stumm, The surface chemistry of oxides, hydroxides and oxide minerals, in: W. Stumm (Editor), Aquatic Surface Chemistry, Wiley-interscience, New York, pp.83-110.

[7] B. Zinder, G. Furrer and W. Stumm, The coordination of weathering: II. Dissolution of Fe(II) oxides, Geochim. Cosmochim. Acta, (1986) *50*, 1861.

[8] B.C. Faust and M.R. Hoffmann, Photoinduced reductive dissolution of α-Fe_2O_3 by bisulfite, Environ. Sci. Technol., (1986) *20*, 943.

[9] S. Banwart, S. Davies and W. Stumm, The reductive dissolution of hematite by ascorbate, Colloid and surfaces, (1988), accepted for publication.

[10] D. Suter, C. Siffert, B. Sulzberger and W. Stumm, Catalytic dissolution of iron(III)(hydr)oxides by oxalic acid in the presence of iron(II), Naturwissenschaften, (1988) *75*, 571.

[11] C. Siffert, PhD thesis, ETH Zurich, in preparation.

[12] R.M. Cornell and P.W. Schindler, Photochemical dissolution of goethite in acid/oxalate solution, Clays and Clay Minerals, (1987) *35*, 347.

[13] B. Sulzberger, D. Suter, C. Siffert, S. Banwart and W. Stumm, Kinetics of dissolution of Fe(III)(hydr)-oxides in natural waters; control by surface coordination, Marine Chemistry, (1988), submitted.

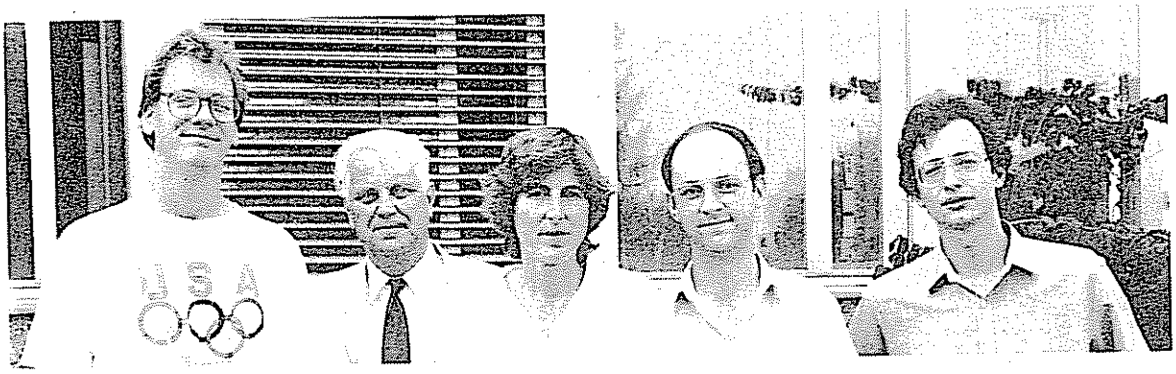

From left to right: Steven Banwart, Werner Stumm, Barbara Sulzberger, Daniel Suter and Christophe Siffert.

GUESTS TO THE EAWAG IN 1988/89

Marijan Ahel, Rudjer Bosković Inst., Zagreb, Yugoslavia
Jorge Bruno, Royal Institute of Technology, Stockholm, Sweden
Silvio Capri, Ist. di Ricerca sulle Acque, Rome, Italy
James Drever, University of Wyoming, USA
Brian Folsom, Washington State University, USA
Michael R. Hoffmann, California Institute of Technology, Pasadena, CA, USA
Maria L.S. Gonçalves, Instituto Superior tecnico, Lisboa, Portugal
Bruce Honeyman, School of Oceanography, University of Washington, USA
Zhang Jian, Eng./Computer scientist, Beijing, China
Bruno Jorge, Royal Institute of Technology, Stockholm, Sweden
James J. Morgan, Caltech, Pasadena, CA
Stephan McDow, Oregon Graduate Center, USA
Carolyn Meyer, Biologist, and Joseph Meyer, University of Wyoming, USA
Manuel Motta, Universidad de Evora, Portugal
Charles O'Melia, Johns Hopkins University, Baltimore, Maryland, USA
Jerald Schnoor, University of Iowa, USA
David van Senden, University of Western Australia, Australia
Aglaia Xyla, University of Patras, Greece
Hanbin Xue, Institute of Environmental Chemistry, Academia Sinica, Beijing, China

EAWAG-PUBLICATIONS

Reprints may be obtained by writing to: EAWAG, Library, CH-8600 Dübendorf

1326
Herczeg, A.L., Imboden, D.M.: Tritium Hydrologic Studies in Four Closed-Basin Lakes in the Great Basin, U.S.A., Limnol.Oceanogr. *33*, 157-173 (1988)

1327
Hoigné, J.: Effect of Abiotic Photochemical Processes on the Chemistry of Aquatic Solutes and on Global Cycles. Appl Geochem. *3*, 63 (1988).

1328
Honeyman, B.D., Balistrieri, L.S., Murray, J.W.: Oceanic Trace Metal Scavenging: the Importance of Particle Concentration. Deep-Sea Res. *35*, 227-246 (1988).

1329
Zeyer, J., Kocher, H.P.: Purification and Characterization of a Bacterial Nitrophenol Oxygenase Which Converts ortho-Nitrophenol to Catechol and Nitrite. J. Bacteriol. *170*, 1789-1794 (1988).

1330
Siegrist, H., Alder, A., Gujer, W., Giger, W.: Behaviour and Modelling of NTA Degradation in Activated Sludge Systems, Water Sci. Techn. *21*, 315-324 (im Druck: 1989).

1331
Xue, H.-B., Stumm, W., Sigg, Laura: The Binding of Heavy Metals to Algal Surfaces. Water Res. 22, 917-926 (1988).

1332
Kohler, H.-P.E.: Isolation of Cobamides from *Methanotrix soehngenii*: 5-Methylbenzimidazole as the α-Ligand of the Predominant Cobamide. Arch. Microbiol. *150*, 219-223 (1988).

1333
Boller, M.: Biologische Phosphorelimination im Belebtschlammverfahren. VSA-Verbandsber. Nr. 344 (1988).

1334
Siegrist, H., Alder, A., Gujer, W., Giger, W.: Verhalten der organischen Komplexbildner NTA und EDTA in Belebungsanlagen. VSA-Verbandsber., Nr. 347 (1988).

1335
Marcomini, A., Giger, W.: Behaviour

of LAS in Sewage Treatment. Changes in the Homologue and Isomer Distributions of Linear Alkylbenzolsulphonates. Tenside-Detergents 25, Oceanogr. *33*, 157-173 (1988)

1336
Hamer, G., Transformation of Nitrogen Compounds in Wastewater Treatment Systems. Abstracts 4th Int. Symp. Microbiol. Ecol., Ljubljana, Yugoslavia, 24.-29.8.1988, pp. 74-79.

1337
Hamer, G.: An Introduction to the Poster Presentations Dealing with the Physiological Modulation of Product Formation. Dechema-Monographs, *105*, 181-184 (1987).

1338
Egli, Th., Wüest, D., Bosshard, Ch., Hamer, G.: the Utilisation of Glucose/Methanol Mixtures by *Hansenula polymorpha* in a Chemostat. Dechema-Monographs, *105*, 225-227 (1987).

1339
Mason, C.A., Hamer, G.: Intra-Cellular Maintenance Requirements and the Extra-Cellular Death/Lysis/Cryptic Growth Cycle. Dechema-Monographs, 105, 285-287 (1987).

1340
Hamer, G., Fleischmann, Th., Mason, C.A.: Aerobic Thermophilic Processes for Waste sewage Sludge treatment: Continuous or Semi-continuous Operation? In : "Continuous Culture" (P. Kyslik & E.A. Dawes, Eds.) Academic Press, London 1988, pp. 71-83.

1341
Honeyman, B.D., Santschi, P.H.: Metals in Aquatic Systems. Environm. Sci. & Technol. *22*, 862-871 (1988).

1342
Marcomini, A., Capel, P.D., Giger, W., Häni, H.: Residues of Detergent-Derived Organic Pollutants and Polychlorinated Biphenyls in Sludge-Amended Soils. Naturwiss., *75*, 460-462 (1988).

1343
Kräutler, B., Kohler, H.-P.E., Stupperich, E.: 5'-Methylbenzimidazolyl-Cobamides are the Corrinoids from some Sulfate-Reducing and Sulfur-Metabolizing Bacteria. Eur. J. Biochem. *176*, 461-469 (1988).

1344
McEvoy, J., Giger, W., Schaffner, C., Ahel, M., Brunner, P.H.: The Occurence of Detergent Derived Organic Micropollutants in Sewage Sludges and Soils Amended with Sludge. In: "Current perspectives in Environmental Biogeochemistry" (G.Giovannozzi-Sermanni and P. Nannipieri, Eds.). NCR—IPRA, Rom 1987, pp. 107-122.

1345
Snozzi, M., Kälin, J.: The Ubiquinol-Cytochrome C Oxidoreductase of Phototrophic Bacteria. In "Cytochrome Systems" (S. Papa, B. Chance and L. Ernster, Eds.), Plenum Publ. Corp., New York 1987, pp. 585-592.

1346
Wieland, E.: Die Verwitterung schwerlöslicher Mineralien- ein koordinationschemischer Ansatz zur Beschreibung der Auflösungskinetik. Diss ETHZ Nr. 8532, Zürich 1988.

1347
Egli, Th., Weilenmann, H.-U., El-Banna, T., Auling, G.: Gram-Negative, Aerobic, Nitrilotriacetate-Utilizing Bacteria from Wastewater and Soil. System. Apll. Microbiol. *10*, 306-312 (1988).

1348
Wehrli, E., Egli, Th.: Morphology of Nitrilotriacetate-Utilizing Bacteria. System. Appl. Microbiol. *10*, 306-312 (1988).

1349
Brunner, P.H.: Approche globale des problèmes d'environnement liés à l'incinération d'ordures ménagères. Pollution Atmosphérique No *119*, 301-308 (1988).

1350
Sulzberger, Barbara, Siffert, Christoph, Stumm, Werner: Oberflächenkoordinations-Chemie und Redox-Prozesse: Zur Auflösung von Eisen(III)-oxiden unter Lichteinfluss. Chimia *42*, 257-261 (1988).

1351
Wieland, E., Wehrli, B., Stumm, W.: the Coordination Chemistry of Weathering: III. A Generalization on the Dissolution Rates of Minerals. Geochim. et Cosmochim. Acta *52*, 1969-1981 (1988).

1352
Capel, P.D., Giger, W., Reichert, P., Wanner, O.: Accidental Input of Pesticides into the Rhine River. Environm. Sci. & Technol. *22*, 992-996 (1988).

1353
Schneider, R.P., Zürcher, F., Egli, Th., Hamer, G.: Determination of Nitrilotriacetate in Biological Matrices Using Ion Exclusion Chromatography. Anal. Biochem. *173*, 278-284 (1988).

1354
Baccini, P., Brunner, P.H.: Neue Ziele für die Abfallwirtschaft. Strategien und Verfahren auf dem Prüfstand. Neue Zürcher Zeitung Nr. 277, 29.9.1988

1355
Bader, H., Sturzenegger, Verena, Hoigné, J.: Photometric Method for the Determination of Low Concentrations of Hydrogen Peroxide by the Peroxidase Catalyzed Oxidation of N,N-Diethyl-p-Phenylenediamine (DPD). Water Res. *22*, 1109-115 (1988).

1356
Stumm, W., Morgan, J.J.: Review about "Aquatic Chemistry; an Introduction Emphasizing Chemical Equilibria in Natural Waters". This Week's Citation Classic, Current Contents Nr. *41*, Oct. 10, 1988, p.18

1357
Kohler, H.-P.E., Kohler-Staub, D., Focht, D.D.: Degradation of 2-Hydroxybiphenyl and 2,2'-Dihydroxybiphenyl by *Pseudomonas sp. Strain HBP1*. Appl.&Environ. Microbiol. *54*, 2683-2688 (1988

1358
Boller, M., Munz, C.: Double Direct Filtration for High Turbidity Removal.

Contents page

Coagulation of Submicron Iron Oxide Particles in Water: Oxide Surface Chemistry in Relation to Particle Kinetics, ***James J. Morgan***, *California Institute of Technology, Caltech, Pasadena, California, USA* 1

The Binding of Heavy Metals to Algal Surfaces, ***Xue Hanbin***, *Research Center for Eco-Environmental Sciences, Academia Sinica, Beijing, People's Republic of China* 3

Fate of Iron and Aluminum in Lake Cristallina, Switzerland, ***Jerald Schnoor***, *Dept. of Civil and Environmental Engineering at the University of Iowa, USA*, ***Rudolf Giovanoli***, *University of Berne, Switzerland*, ***Laura Sigg, Werner Stumm, Barbara Sulzberger, Jürg Zobrist*** 5

Participants of the Nineth Postgraduate Course in Sanitary Engineering and Water Pollution Control 9

Colloidal Stability and Eutrophication, ***Charles O'Melia***, *Department of Geography and Environmental Engineering, Johns Hopkins University, Baltimore, Maryland, USA* 10

The Influence of Ammonia on the Oxidation of Aqueous Sulfur Dioxide in Atmospheric Deposition, ***Philippe Behra, Laura Sigg, Werner Stumm*** 12

Kinetics of Dissolution of Fe(III)-Oxides in Natural Waters, ***Barbara Sulzberger, Steven Banwart, Christophe Siffert, Daniel Suter, Werner Stumm*** 18

Publications 1326-66 23

In: "Particle Technology in Relation to Filtration and Separation" (A. Faseur & R. de Bruyns, Eds.). 391st Event of Eur. Fed. Chem. Engineers, Antwerp, Belgium 1988, pp.31.-38.

1359
Mechsner, Kl.: Gesetzliche Aspekte der Umweltbelastungen durch Reinigungs-und Desinfektionsmittel. In: "Reinigung und Desinfektion im Lebensmittelbereich". Schriften-Lebensmittelbereich". Schriftenreihe. Schweiz. Ges. Lebensmittelhygiene H. *18* (Vortr. 21. Arb.tagung, 24.11.1988).

1360
Al-Awadhi, N., Egli, Th., Hamer, G.: Growth Characteristics of a Thermotolerant Methylotrophic *Bacillus sp (NCIB 12522)* in Batch Culture. Appl. Microbiol. Biotechnol. *29*, 485-493 (1988)

1361
Baccini, P., Brunner, P.H.: Sortierung in der Abfallwirtschaft: Wie gross ist ihr Beitrag zu einem ressourcenschonenden und umweltverträglichen Stoffhaushalt? Gas-Wasser-Abwasser 68, 617-622 (1988)

1362
Sieber, U.W.: Untersuchungen zur Oekologie der Ciliaten der Klasse Oligohymenophora in einem schweizerischen Fliessgewässer (Thur). Diss. ETHZ Nr. 8564, Zürich 1988.

1363
Boller, M.: Versickerung von Meteorwasser und Abwasser. VSA-Verbandsber. Nr. 372 (1988).

1363
Suter, D., Siffert, Chr., Sulzberger, Barbara, Stumm, W.: Catalytic Dissolution of Iron(III)(Hydr)oxides by Oxalic Acid in the Presence of Fe(II). Naturwiss. *75*, 571-573 (1988)

1365
Santschi, P.H.: Factors Controlling the Biogeochemical Cycles of Trace Elements in Fresh and Coastal Marine Waters as Revealed by Artificial Radioisotopes. Limnol. Oceanogr. *33*, 848-866 (1988).

1366
Ruzič, I., Ulrich, H.J., Cosovič, Bozena: Time Dependence of The Adsorption of Valeric Acid at the Mercury-Sodium Chloride Interface. J. Colloid & Interface Sci. *126*, 525-536 (1988).

Impressum

Printed: *on 100% recycled paper, i.e. with very little water consumption, no bleaching and no coloration.*
Editor: *Diana Hornung, EAWAG*

Subscription for EAWAG-News
New subscribers are welcome: the English edition appears annually in summer, the French/German version is available twice a year. Please complete this subscription form and return it

TO THE LIBRARY,
EAWAG, 8600 DÜBENDORF, SWITZERLAND

Full Mailing Address: Name/Title: ____________________
Position/Company/Institute: ____________________

☐ Note the following change of address ____________________
Please send me regularly the EAWAG-News in ____________________
☐ English ☐ French/German ____________________

☐ Please send me the following reprints ____________________
____________________ ____________________